Pavia, June 12th 2025

# The X17 , a new particle Beyond the Standard Model ?
# The MEG II experiment result in the quest for an experimental confirmation

Gianluigi Boca

# The ATOMKI anomalies

At the ATOMKI laboratory, Debrecen, Hungary an anomalous distribution of the angle between the electron and the positron was reported in three different nuclear reactions, **possibly caused by a new particle, X17, of mass about 17 MeV**.

$^{7}\mathrm{Li} + \mathrm{p} \rightarrow {}^{8}\mathrm{Be}^{*} \rightarrow {}^{8}\mathrm{Be}\ e^{+}e^{-}$ A.J. Krasznahorkay et al. PRL 116, 042501 (2016)

$^{3}\mathrm{H} + \mathrm{p} \rightarrow {}^{4}\mathrm{He}^{*} \rightarrow {}^{4}\mathrm{He}\ e^{+}e^{-}$ A.J. Krasznahorkay et al. Phys. Rev. C 104, 044003 (2021)

$^{11}\mathrm{B} + \mathrm{p} \rightarrow {}^{12}\mathrm{C}^{*} \rightarrow {}^{12}\mathrm{C}\ e^{+}e^{-}$ A.J. Krasznahorkay et al. Phys. Rev. C 106, L061601 (2022)

# The ATOMKI anomaly in $^{7}Li + p \rightarrow {}^{8}Be\ e^{+}e^{-}$

reported in 2016 (and with an improved setup in 2018)

**Brief summary of the $^{7}Li + p$ reactions of interest here**

Direct proton capture : $^{7}Li + p \rightarrow {}^{8}Be\ \gamma$

Production of **Be* intermediate excited states** :

$$^{7}Li + p \rightarrow {}^{8}Be^{*}$$

# Be* excited states, $^{7}Li + p \rightarrow {}^{8}Be^{*} \rightarrow {}^{8}Be\ \gamma$ cross section

$^{7}Li + p$ can form many $^{8}Be^{*}$ excited states, depending on the p energy

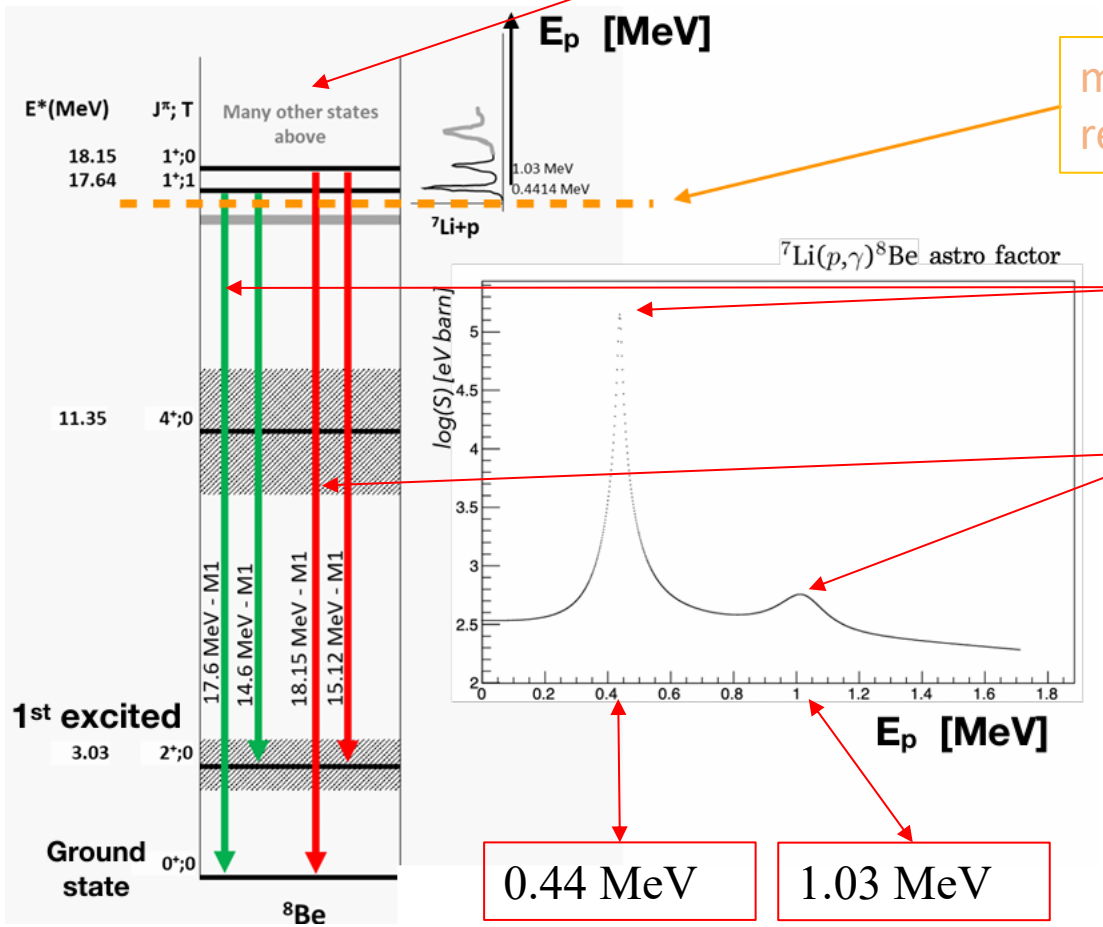


minimum energy level reached in $^{7}Li + p$

$^{8}Be^{*}$ 17.6 MeV
$J^{P} = 1^{+}$ excited state

$^{8}Be^{*}$ 18.1 MeV
$J^{P} = 1^{+}$ excited state

0.44 MeV

1.03 MeV

**astro factor** $\mathbf{S \equiv E_p\, \sigma(Ep)_{effective}}$ where $E_p$ = proton kinetic energy, $\boldsymbol{\sigma(Ep)_{effective}}$ is the cross section, and $\boldsymbol{\sigma(Ep)_{effective} \equiv \tau(E_p)\, \sigma(Ep)}$ where $\tau(E_p) \equiv$ transparency of the coulombian barrier, and $\sigma(E_p) \equiv$ nuclear cross section

# Be* excited states

The $^{8}Be^{*}$ excited states can decay strongly :

$^{8}Be^{*} \rightarrow {}^{7}Li + p$ $^{8}Be^{*} \rightarrow {}^{7}Be + n$

$^{8}Be^{*} \rightarrow {}^{6}Li + d$ $^{8}Be^{*} \rightarrow \alpha + \alpha$

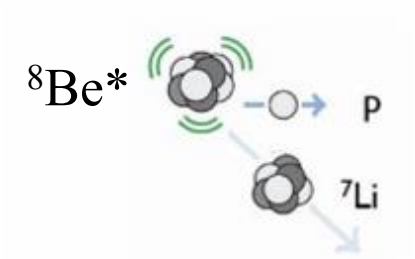


The $^{8}Be^{*}$ excited states can decay electromagnetically :

$^{8}Be^{*} \rightarrow \gamma\ {}^{8}Be$ (or $^{8}Be^{*\prime}$ )

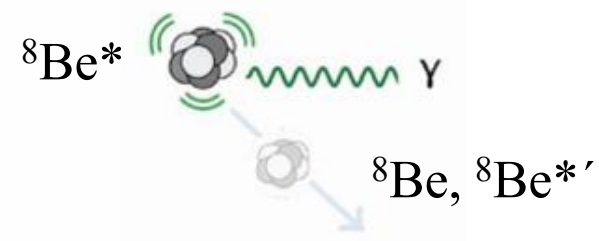


or

**$^{8}Be^{*} \rightarrow {}^{8}Be$ (or $^{8}Be^{*\prime}$) $\gamma^{*}$** with $\gamma^{*} \rightarrow e^{+}e^{-}$
**Internal Pair Conversion (IPC)**

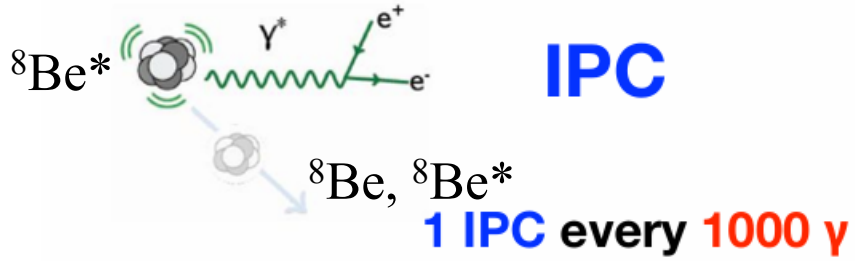

# The ATOMKI anomaly in $^7$Li + p → $^8$Be $e^+e^-$

**ATOMKI found an anomalous distribution in the angle between $e^+$ and $e^-$ in $^7$Li + p → $^8$Be*(18.1 MeV, $J^P = 1^+$) → $^8$Be ($J^P = 0^+$) $e^+e^-$**

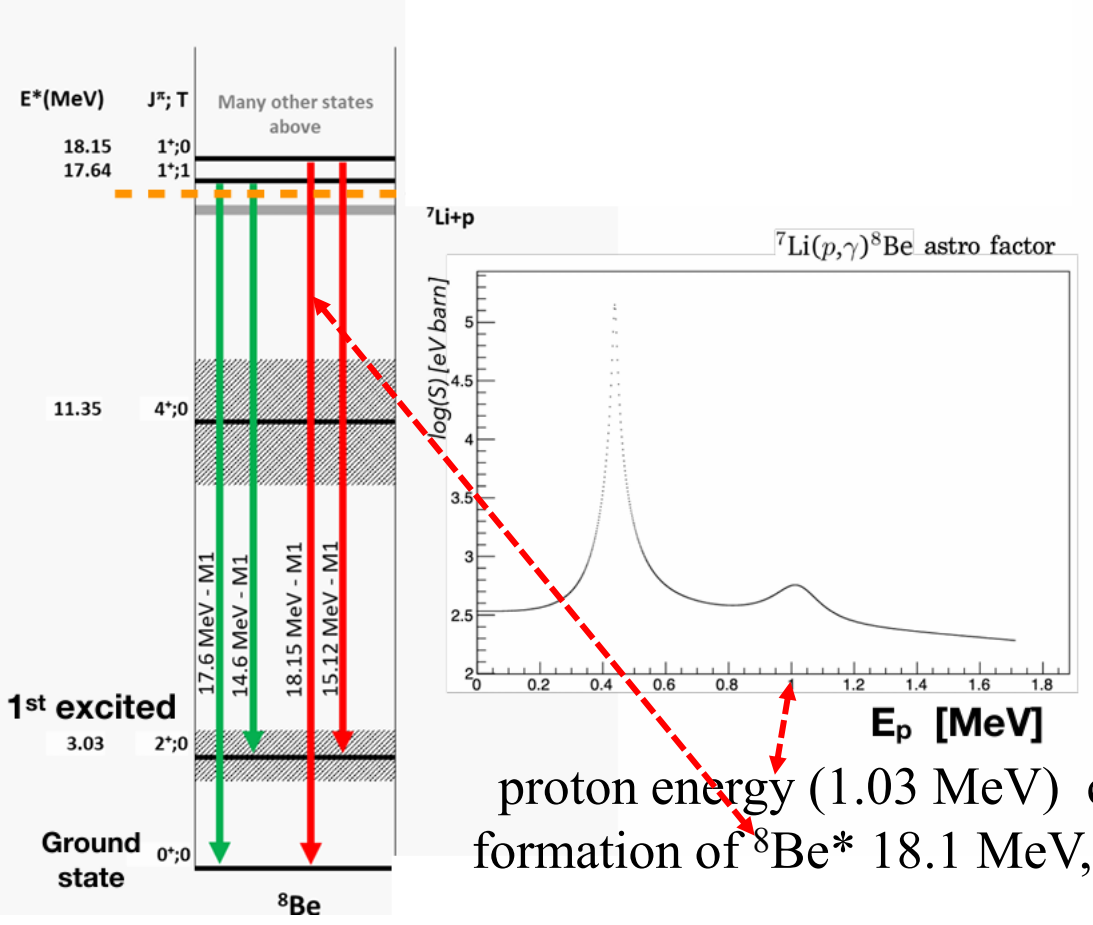





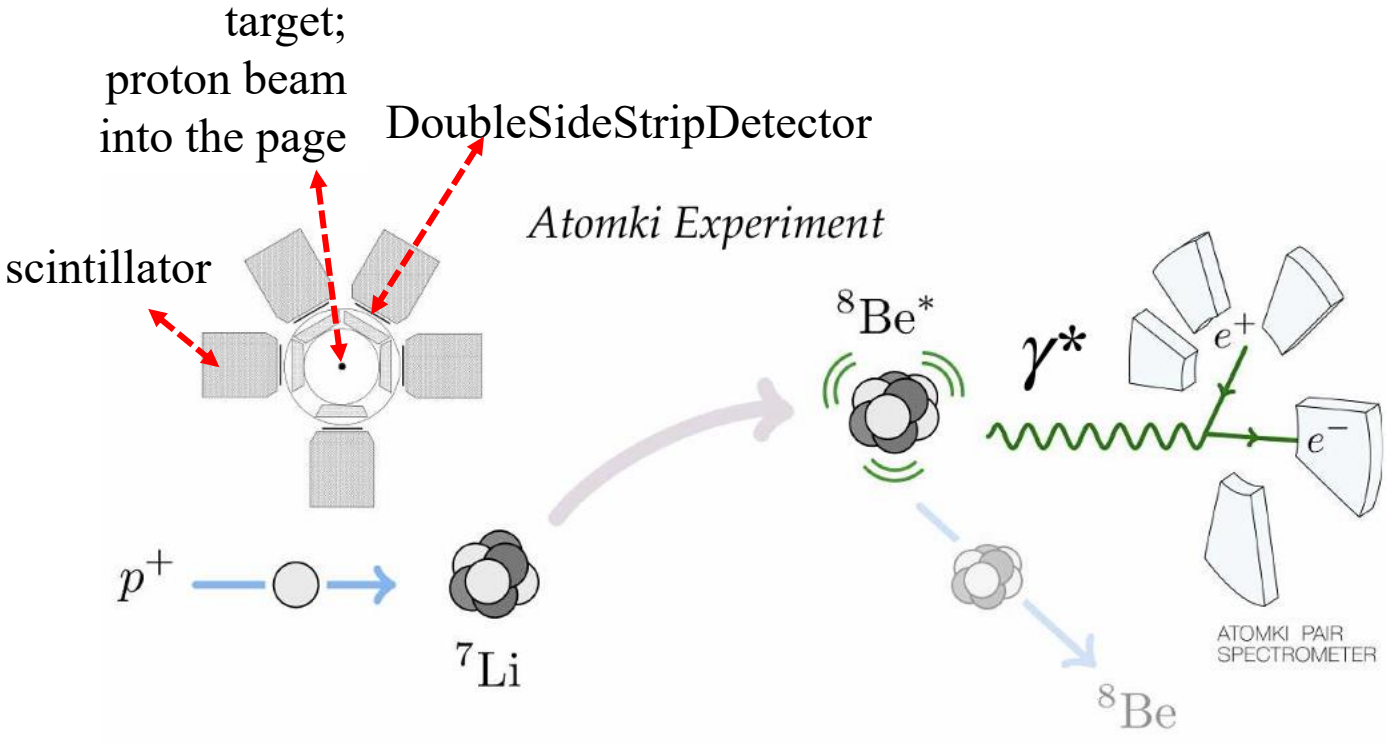


proton energy (1.03 MeV) corresponding to the formation of $^8$Be* 18.1 MeV, $J^P = 1^+$ excited state

# The ATOMKI anomaly in $^{7}Li + p \rightarrow {}^{8}Be\ e^{+}e^{-}$

The anomaly was an excess of events in the angle Θ between $e^+$ and $e^-$ around 140 degrees for beam proton energies near the excitation of the $^{8}Be^{*}$(18.1 MeV) state ($E_p$ = 1.03 MeV).
**This transition goes from a $J^P = 1^+$ state to a $J^P = 0^+$ state**

Such a distribution could not be described by the known IPC theory predictions (continuos curves)

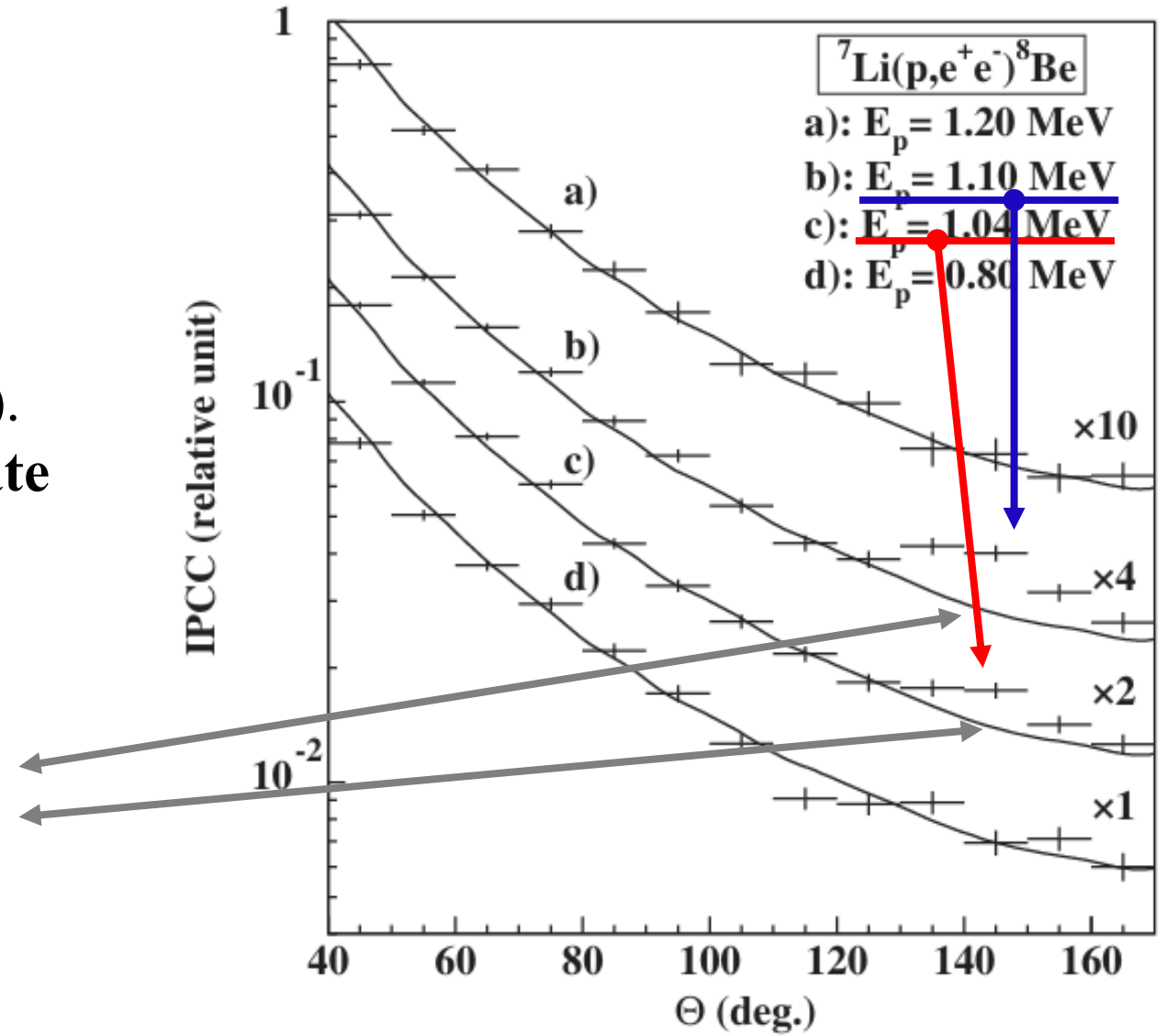

# Small summary of the known IPC theory for $^7$Li + p → $^8$Be $e^+e^-$

In all the IPC models, the $^7$Li + p → $^8$Be $e^+e^-$ cross section is intimately connected to the $^7$Li + p → $^8$Be $\gamma$ process.

The $^7$Li + p → $^8$Be $\gamma$ cross section is described in terms of **multipole contributions** of the nuclear electromagnetic field $A^\mu$

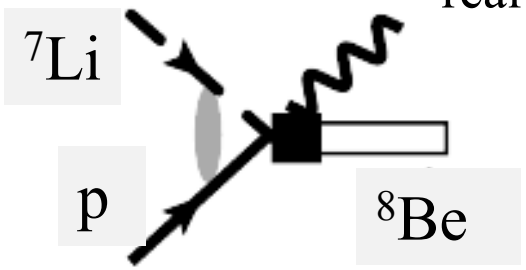


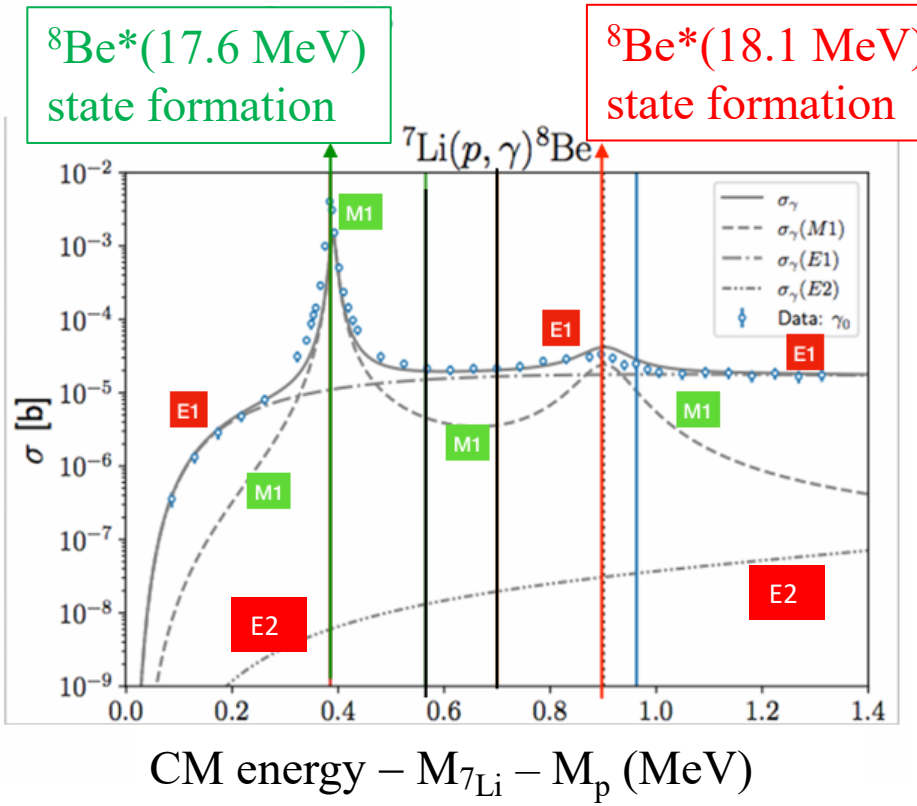


**Gysbers et al, Phys.Rev. C 110, 015503 (2024)**

M1 magnetic dipole contribution

E1 electric dipole contribution

E2 electric quadrupole contribution

The $^8$Be*(18.1 MeV) and the $^8$Be*(17.6 MeV) de-excitations with γ emission are M1 transitions

The **continuum p-capture** with γ emission is a E1 transition

The two contributions interfere.

# Little summary of the known IPC theory for $^7$Li + p → $^8$Be $e^+e^-$

In all the IPC models, the $^7$Li + p → $^8$Be $e^+e^-$ cross section is intimately connected to the $^7$Li + p → $^8$Be $\gamma$ process.

The IPC $^7$Li + p → $^8$Be $e^+e^-$ is obtained in the various models by coupling a $e^+e^-$ **current** operator to the **EM multipolar field** operator.

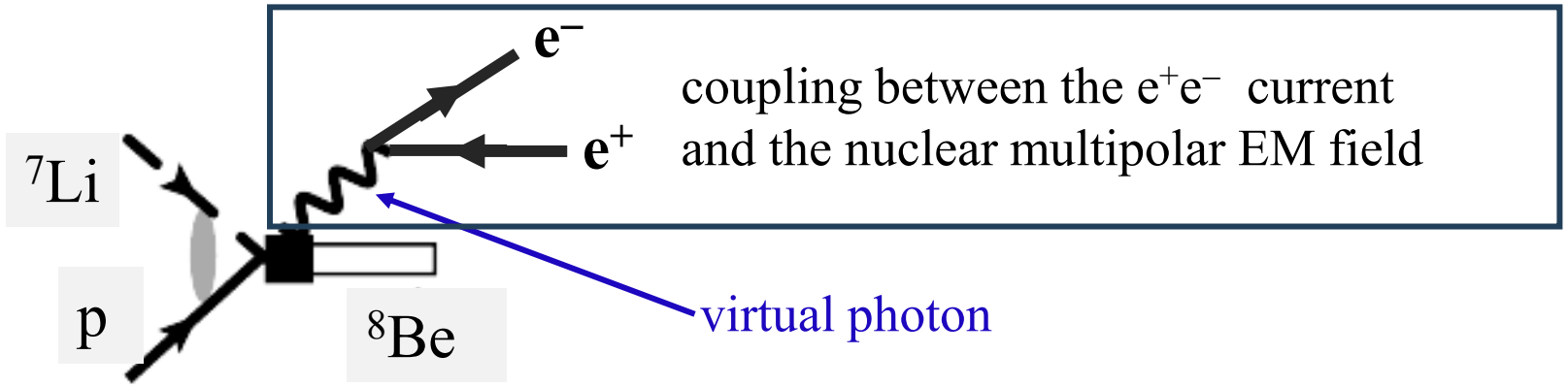


That boils down to the presence of extra multiplicative terms $\bar{u}_{s-}(\vec{p}_-)ie\gamma_\mu v_{s+}(\vec{p}_+)A^\mu$

in the transition matrix : $\bar{u}_{s-}(\vec{p}_-)\equiv$ Dirac electron spinor $v_{s+}(\vec{p}_+)\equiv$ Dirac positron spinor

$A^\mu\equiv$ nuclear EM field $\gamma_\mu\equiv$ Dirac matrix $e\equiv$ electron charge

That's why also the $^7$Li + p → $^8$Be $e^+e^-$ process is described in terms of EM multipoles contributions and the shape of the cross section is similar to the shape of $^7$Li + p → $^8$Be $\gamma$

# The Gysbers et al. IPC model for $^{7}Li + p \rightarrow {}^{8}Be\ e^{+}e^{-}$

**Gysbers et al, Phys.Rev. C 110, 015503 (2024)**

**Ab initio** calculation including the possibility of **interference** between E1, E2 and M1 multipolarities of the nuclear electromagnetic field operators. The shape of $\sigma(^{7}Li\ p \rightarrow {}^{8}Be\ e^{+}e^{-})$ is similar to the shape of $\sigma(^{7}Li\ p \rightarrow {}^{8}Be\ \gamma)$

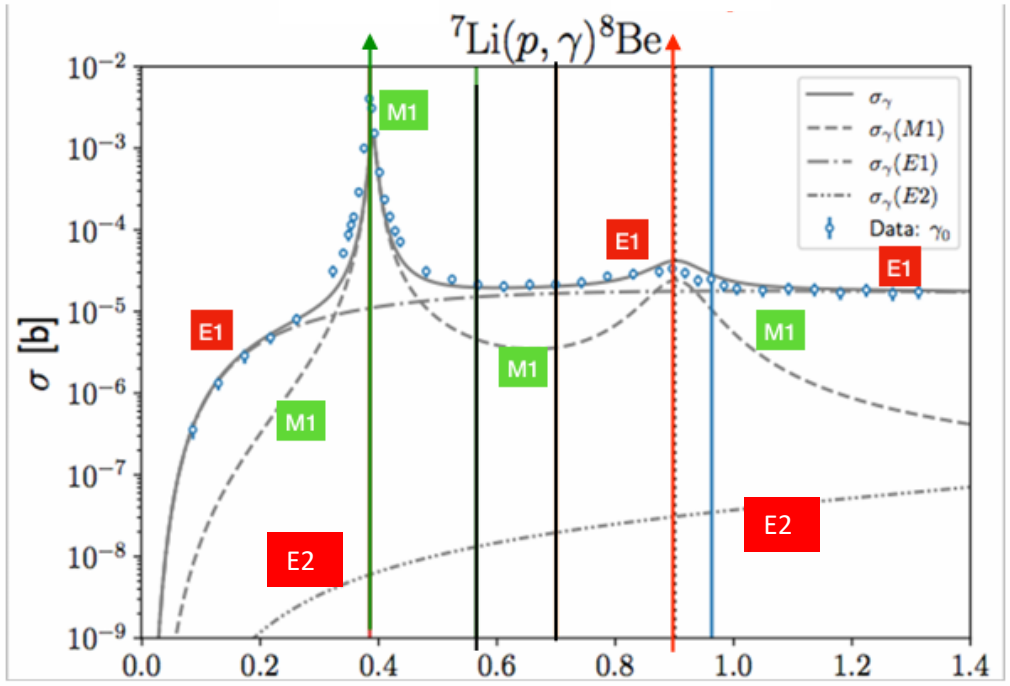


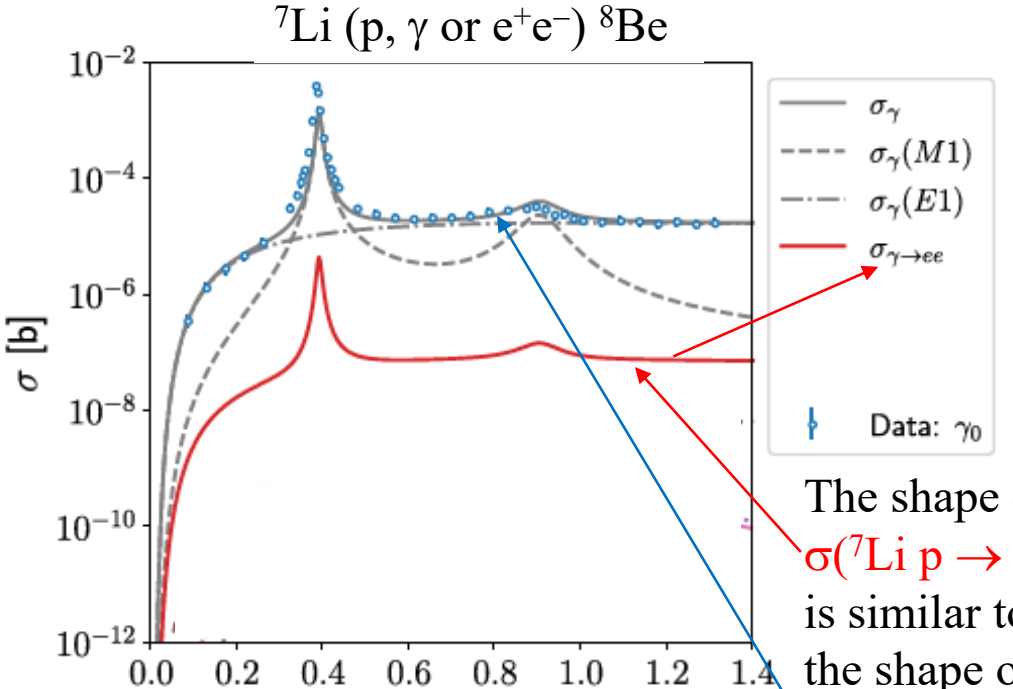


The shape of the of $\sigma(^{7}Li\ p \rightarrow {}^{8}Be\ e^{+}e^{-})$ is similar to the shape of $\sigma(^{7}Li\ p \rightarrow {}^{8}Be\ \gamma)$

# The Rose IPC model for $^{7}Li + p \rightarrow {}^{8}Be\ e^{+}e^{-}$

**M.E.Rose, Phys.Rew. 76, N.5, 67 (1949)**

$$d_{IPC} \propto p_{+}p_{-}W_{+}W_{-} \sum_{s+s-} |(\psi_{-}[V + \boldsymbol{\alpha} \cdot \boldsymbol{A}]\psi_{+})|^{2} d\Omega_{+} d\Omega_{-} dW_{+}$$

$d_{IPC}$ = pair decay rate

$p_{+}\ p_{-} \equiv$ positron/electron 3-momentum

$s+\ s- =$ positron/electron spin

$W_{+}\ W_{-} \equiv$ positron/electron energy

$\psi_{-} \equiv$ free electron Dirac wave function

$\psi_{+} \equiv$ free positron Dirac wave function

$V, \boldsymbol{A} \equiv$ electromagnetic field

$d\Omega_{+} d\Omega_{-} \equiv$ positron/electron solid angle

$\boldsymbol{\alpha} \equiv$ three matrices of the Dirac equation

$dW_{+} \equiv$ positron energy range between $W_{+}$ and $W_{+} + dW_{+}$

This model describes the production of a an e+e- pair via the interaction of the nuclear electromagnetic field of a given multipolarity (E1, M1, etc). **No interference** among different multipolarities.

# The Zhang-Miller IPC model for $^{7}Li + p \rightarrow {}^{8}Be\ e^{+}e^{-}$

**X.Zhang and G.A.Miller, Phys.Lett. B 773, 165 (2017)**

**Effective Field model** including the possibility of **interference** between E1, E2 and M1 multipolarities of the nuclear electromagnetic field operators

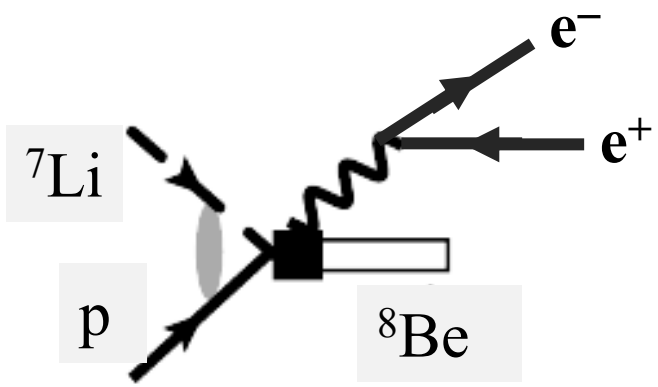


'non-resonant' proton capture, E1, E2 only; dominated by E1

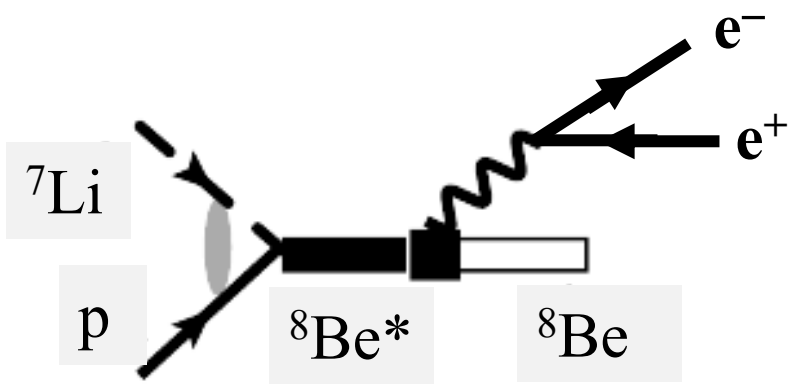


'resonant' proton capture, via the $^{8}Be^{*}$ excited state; M1 dominated

# The ATOMKI anomaly in $^7$Li + p → $^8$Be $e^+e^-$

**None of the known IPC calculations could fit the anomaly.**

**A possible alternative explanation** : a new boson particle (possibly with **$J^P = 1^+$ like an axion**) is produced as an intermediate step of the reaction $^7$Li + p and the boson decays into $e^+e^-$ isotropically

$$^7\text{Li} + \text{p} \rightarrow {}^8\text{Be} + \text{X17} \quad \text{with} \quad \text{X17} \rightarrow e^+e^-$$

From their best fit (in 2016):

$M_{X17} = 16.70 \pm 0.35 \pm 0.5$ MeV/c²

$$\frac{\text{BR}(^8\text{Be} + \text{X17})}{\text{BR}(^8\text{Be}^*(18.1) \rightarrow {}^8\text{Be}\ \gamma)} = 5.8 \times 10^{-6}$$

with an improved setup (in 2018):

$M_{X17} = 17.01 \pm 0.16$ MeV/c²

$$\frac{\text{BR}(^8\text{Be} + \text{X17})}{\text{BR}(^8\text{Be}^*(18.1) \rightarrow {}^8\text{Be}\ \gamma)} = (6 \pm 1) \times 10^{-6}$$

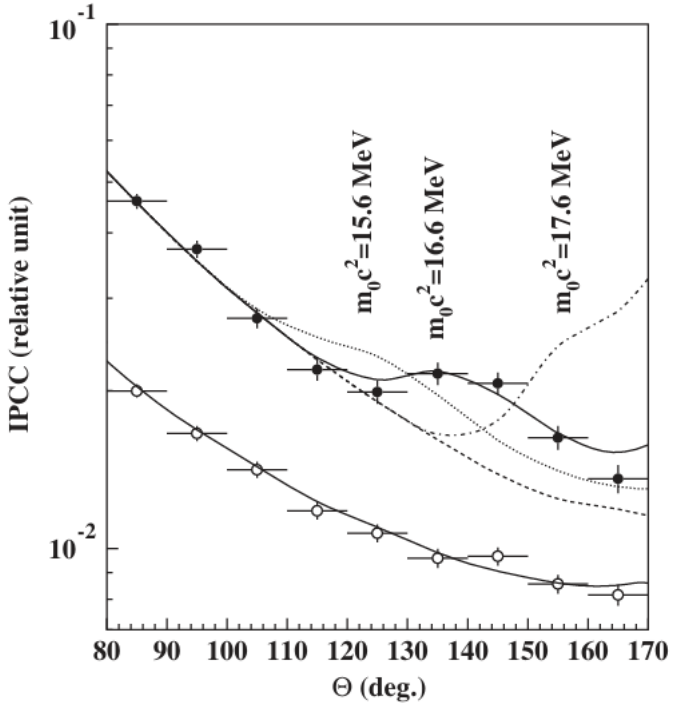


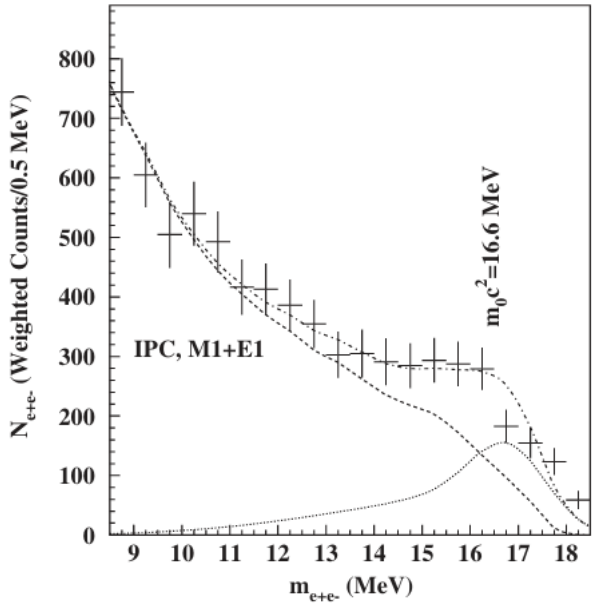

# The ATOMKI anomaly in $^3H + p \rightarrow {}^4He\ e^+e^-$

reported in 2021

The experiment was repeated with a Tritium target and with an improved setup, at different proton energies

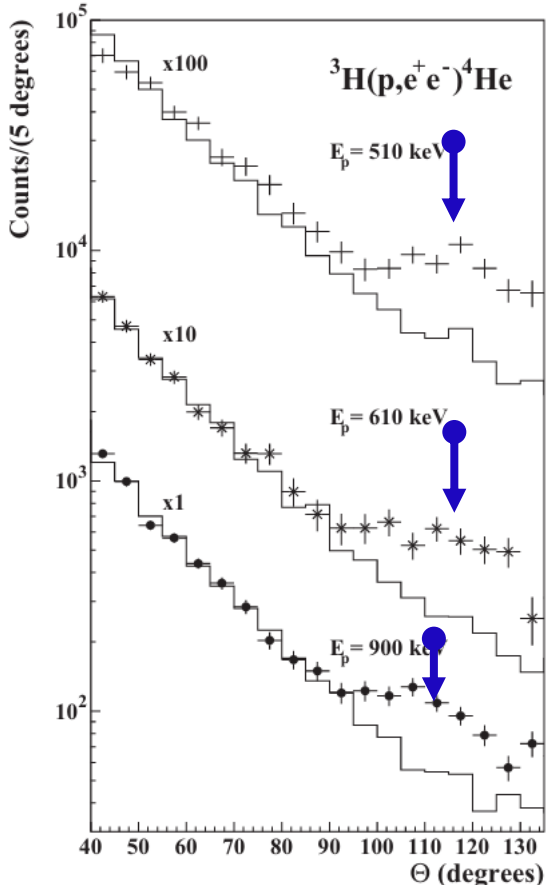


again they could not reproduce the event excess at different $E_p$ energies for angles between $e^+$ and $e^-$ around 110 degrees with the IPC distribution + background produced by γ converting into $e^+$ $e^-$ in the detector material

**(≡ EPC = External Pair Conversion)**

$$M_{X17}=16.94\pm0.12\pm0.21\ \text{MeV}/c^2$$

$$\frac{BR(^4He + X17)}{BR(^4He^* \rightarrow {}^4He\ \gamma)}=(5.1\pm0.13)\times10^{-6}$$

# The ATOMKI anomaly in $^{11}B + p \rightarrow {}^{12}C\ e^+\ e^-$

reported in 2022

The experiment was also repeated with a Boron target at different proton energies

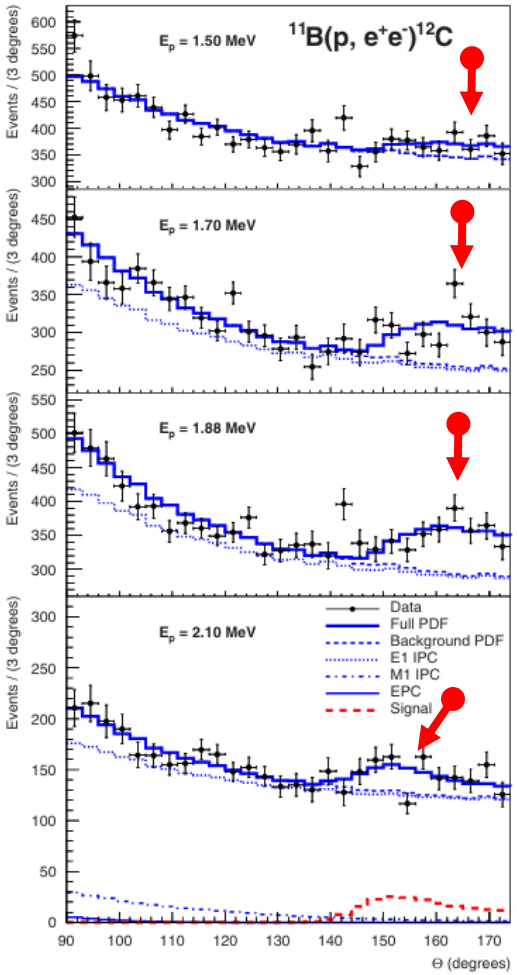


again they could not reproduce the event excess at different $E_p$ energies for angles between $e^+$ and $e^-$ greater than 140 degrees with the IPC distribution + background EPC

$$M_{X17} = 17.03 \pm 0.11 \pm 0.20 \quad \text{MeV/c}^2$$

$$\frac{BR(^{12}C + X17)}{BR(^{12}C^*(17.23) \rightarrow {}^{12}C\ \gamma)} = (3.6 \pm 0.3) \times 10^{-6}$$

# ….. any evidence from other experiments?

No evidence from NA48/2 in $\pi^0 \rightarrow \gamma\, e^+e^-$ (Phys.Lett. B 746,178, 2015)

No evidence from NA64 in $e^- Z \rightarrow e^- Z\, e^+e^-$ (Phys.Rev.D 101:071101 2020)

where Z means an active target (calorimeter). The $e^-$ energy was 150 GeV

> 4 σ evidence claimed in $^7Li + p \rightarrow {}^8Be + e^+e^-$ by Tran The Anh *et al.* in an experiment performed at Vietnam National University, Hanoi (arXiv:2401.11676v2, 2024)

**$M_{X17} = 16.66 \pm 0.47 \pm 0.35$ MeV**

**However the energy of the production is higher than that of the Be* (18.1 MeV) excited state.** The energy of the incident proton was 1.225 MeV (instead of the 1.03 MeV).

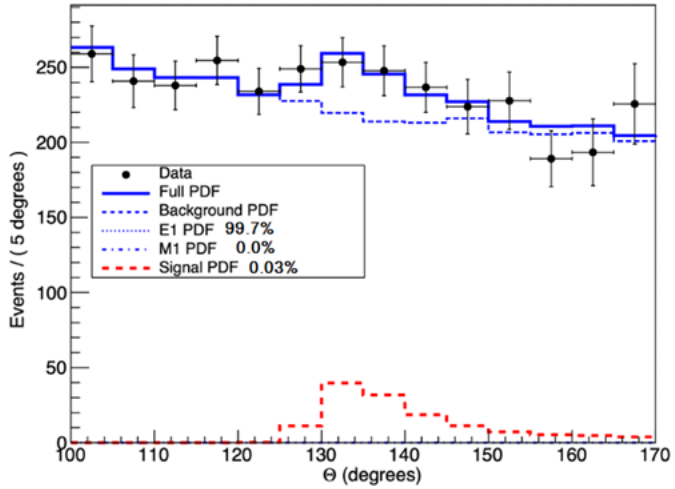

# ….. any evidence from other experiments?

Recent result from PADME (at Frascati) in the s-channel : $e^+e^- \rightarrow X17 \rightarrow e^+e^-$
(Light Dark Matter @ Accelerators international workshop, Genova, 8-11 April 2025)

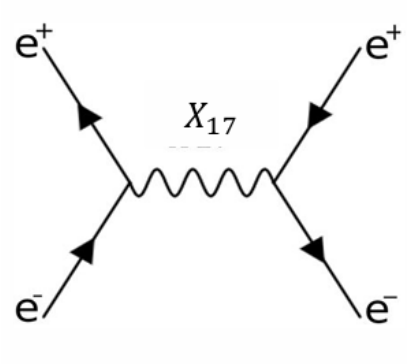


$$\underbrace{N_2(s) \,/\, ( N_{POT}(s)\, B(s) )}_{g_R(s)} = [\, 1 + S(s; M_X, g)\, \varepsilon_S(s) \,/\, B(s) \,]$$

- $N_{POT}(s)$ number of e+ on target from beam-catcher calorimeter
- $B(s)$ background yield expected per POT
- $S(s; M_X, g)$ signal production expected per POT for {mass, coupling} = {$M_X$, g}
- $\varepsilon_S(s)$ signal acceptance and selection efficiency

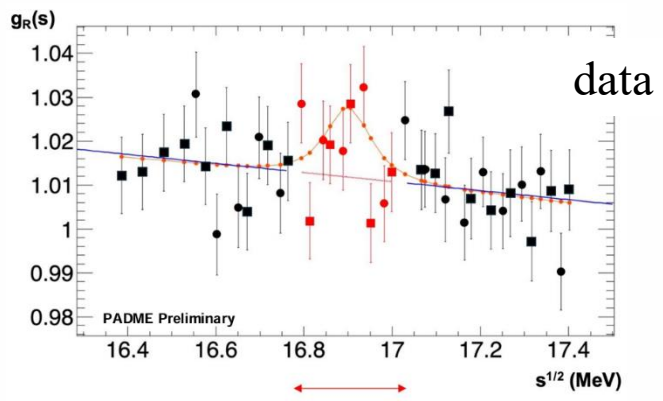


data

**PADME conclusion:**
**'No indications of X17 signal beyond 2 sigma-equivalent global p-values'**

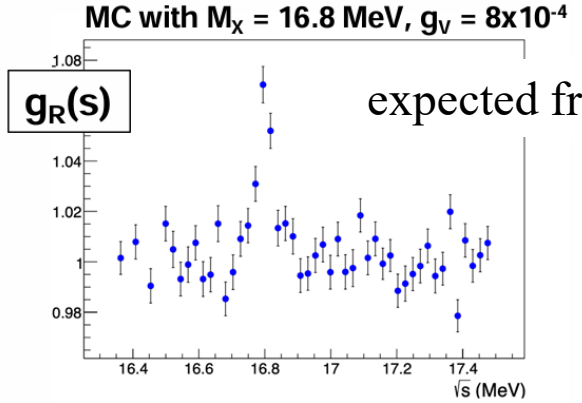


expected from MC

# A new particle discovered?

**Today we think the Standard Model is not THE fundamental theory and a higher simmetry theory might exist**

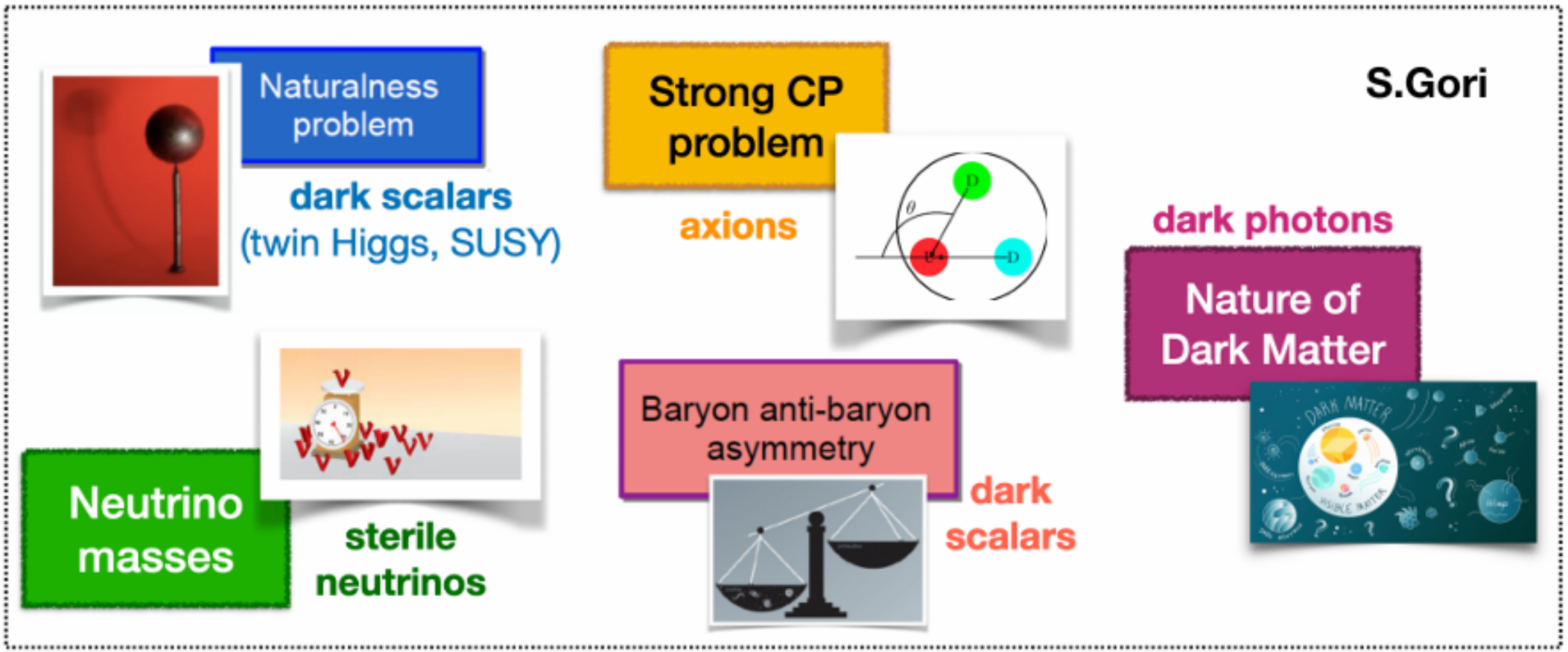

# X17, a new particle discovered?

It could be a sign of new physics

Could the X17 be the axion long sought for the CP strong problem ?
Could it belong to the Dark Matter sector?

**A confirmation by another experiment is necessary !**

The MEG II apparatus has the possibility to repeat the

$$^{7}\mathrm{Li} + \mathrm{p} \rightarrow {}^{8}\mathrm{Be}\ e^{+}e^{-}$$

experiment

MEGII was originally designed for CLFV search. Data taking is still ongoing.
Current best limit : $\mathrm{BR}(\mu^{+} \rightarrow e^{+}\gamma) < 1.5 \times 10^{-13}$ , 90% C.L. EPJ C 84, 216 (2024)

# The MEG II apparatus at PSI for the $\mu^+ \rightarrow e^+\gamma$ search

900L LXe tank, readout by 668 PMTs and 4092 SiPMs, resolution = 2.0/1.8 % at $E_\gamma$ = 55 MeV

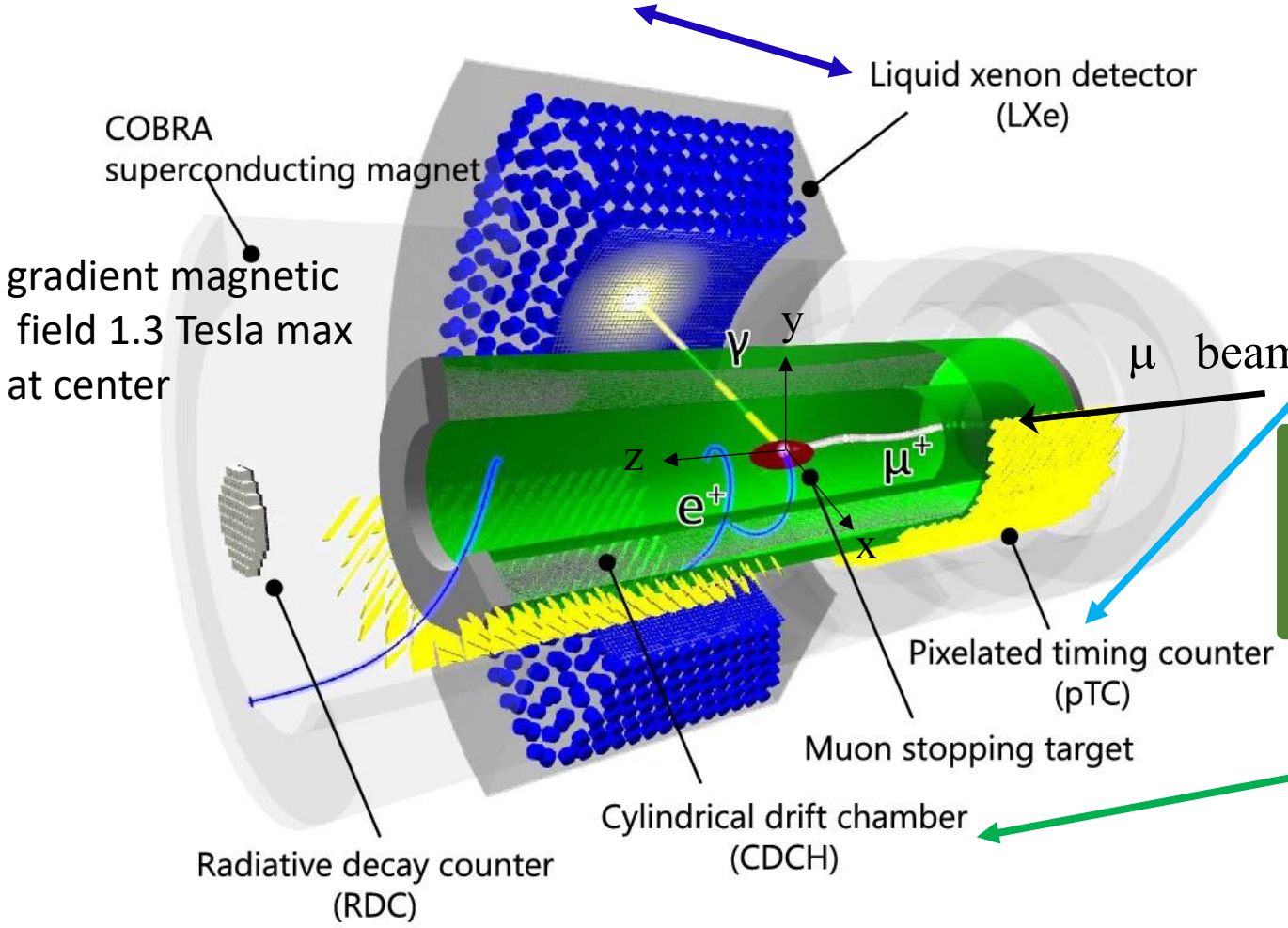


**pTC** : 512 plastic tiles, 35 ps resolution on the positron track time of passage

- single volume : He-isobutane-isopropyl alchol-$O_2$
- 9 concentric layers of 192 cells each
- momentum resolution : 90 keV at $E_e \sim 52$ MeV

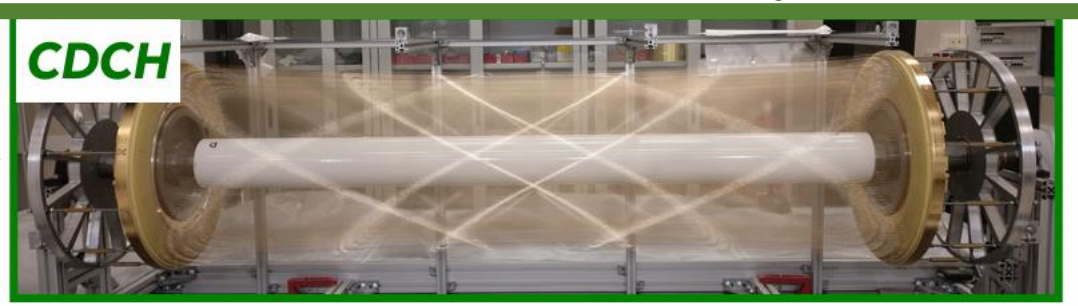

# The MEG II apparatus for the $^7Li + p \rightarrow {}^8Be$ X17 search

## the proton beam

Produced by a Cockroft-Walton normally used for calibration of the Liquid Xenon detector with the $^7Li + p \rightarrow {}^8Be^*(17.6\ MeV) \rightarrow {}^8Be\ \gamma(17.6\ MeV)$ reaction, at $E_p = 0.44$ MeV

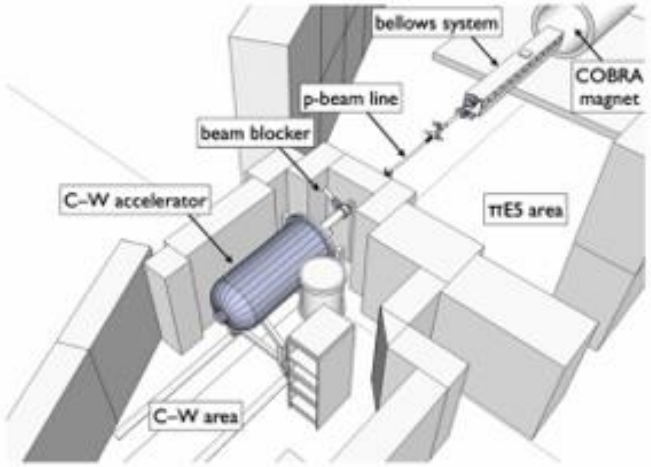


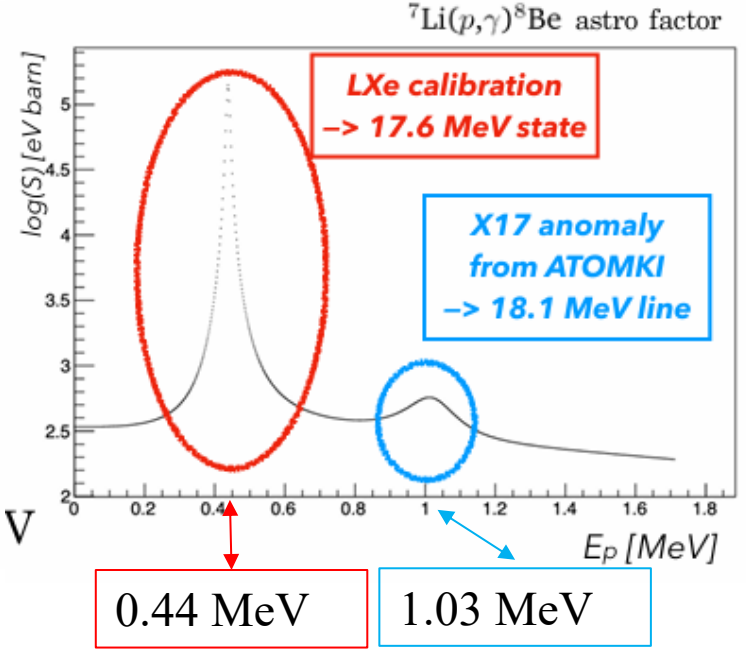


For the X17 campaign the proton energy was raised **up to 1.08 MeV**, with a proton current of up 10 μA impinging on a LiPON Lithium Phosphorous Oxynitride ($Li_{3-x}PO_{4-y}N_{x+y}$) on Cu substrate target

# The MEG II apparatus for the $^{7}Li + p \rightarrow {}^{8}Be$ X17 search

## the proton beam

proton beam at ~ 1.08 MeV from a Cockroft-Walton. It enter the apparatus from the opposite side with respect to the muon beam

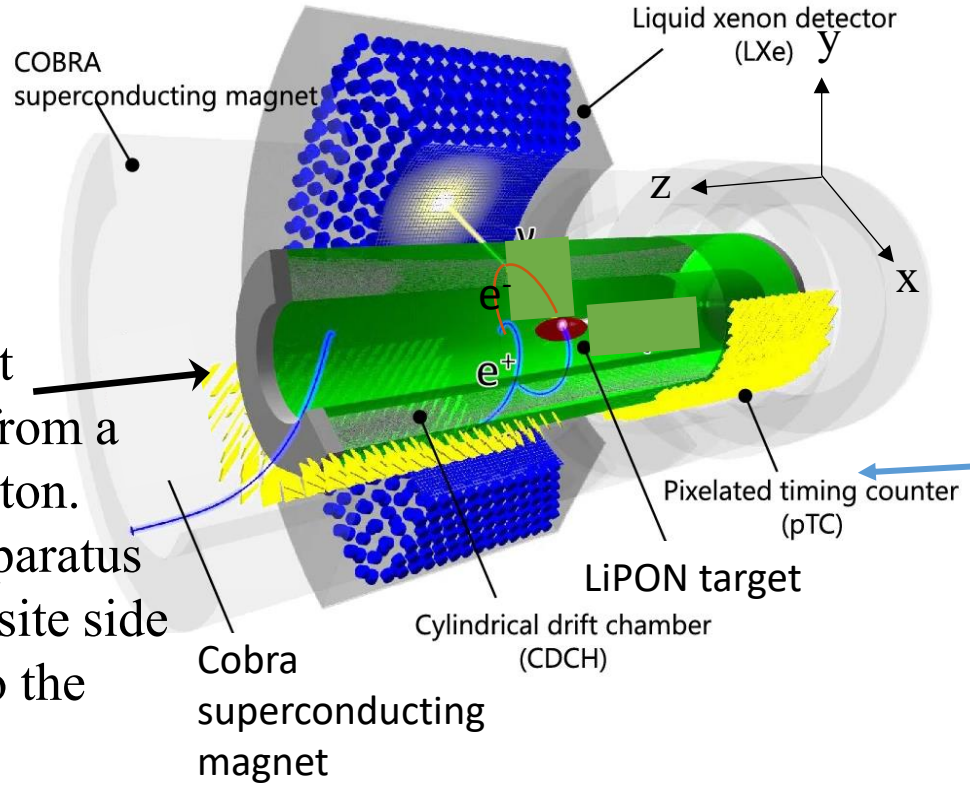


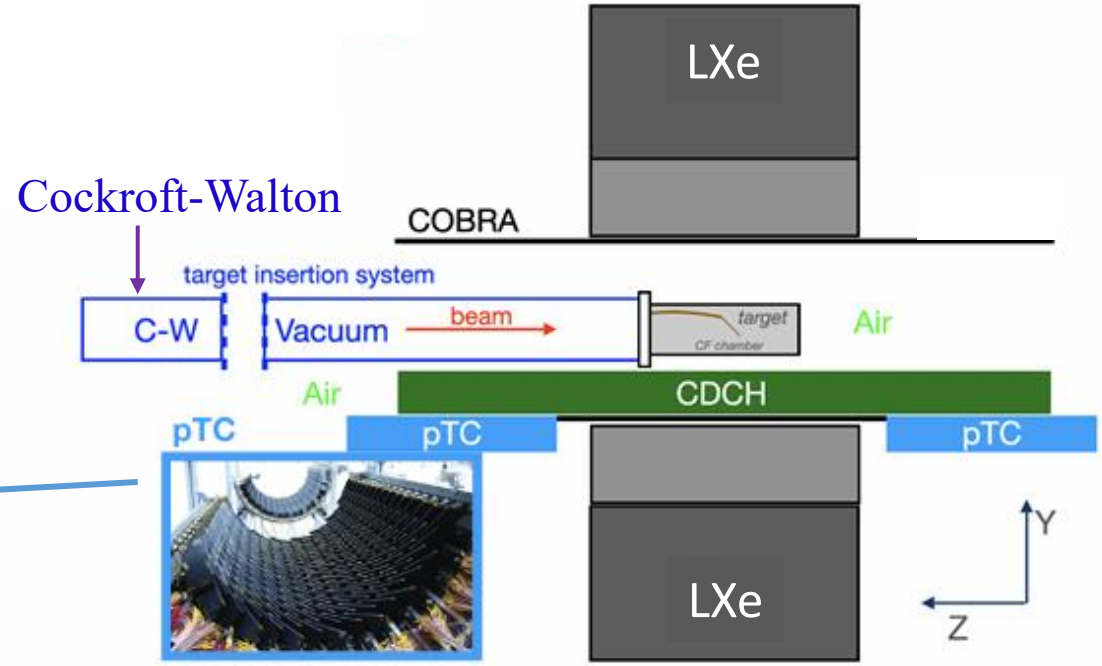


side view

# The MEG II apparatus for the $^{7}Li + p \rightarrow {}^{8}Be$ X17 search

## the proton beam

During the Feb 2023 four weeks data taking, the beam was composed by **75% $H^+$** and **25% $H_2^+$** ions with kinetic energy **1.08 MeV** . Consequently protons of **$H_2^+$** interacted with kinetic energy of **0.54 MeV** only.

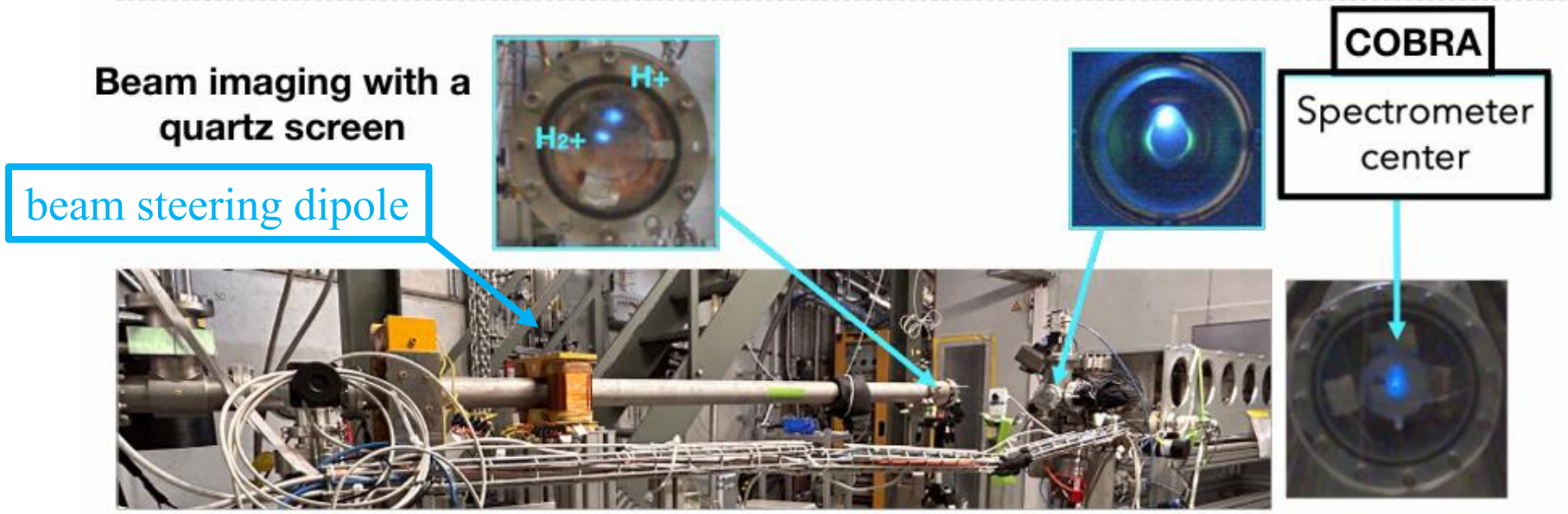


the Cockroft-Walton beam line

# Reaction channels detected by MEG II

Both the **18.1 MeV excited state** (by $H^+$ , $E_p$~1.08 MeV) and the **17.6 MeV excited states** (by $H_2^+$ , $E_p \leq 0.54$ MeV ) were formed, plus possibly a non-resonant contribution **(direct proton capture)** due to incident proton energy loss in the target before interaction

$E_p \equiv$ proton kinetic energy

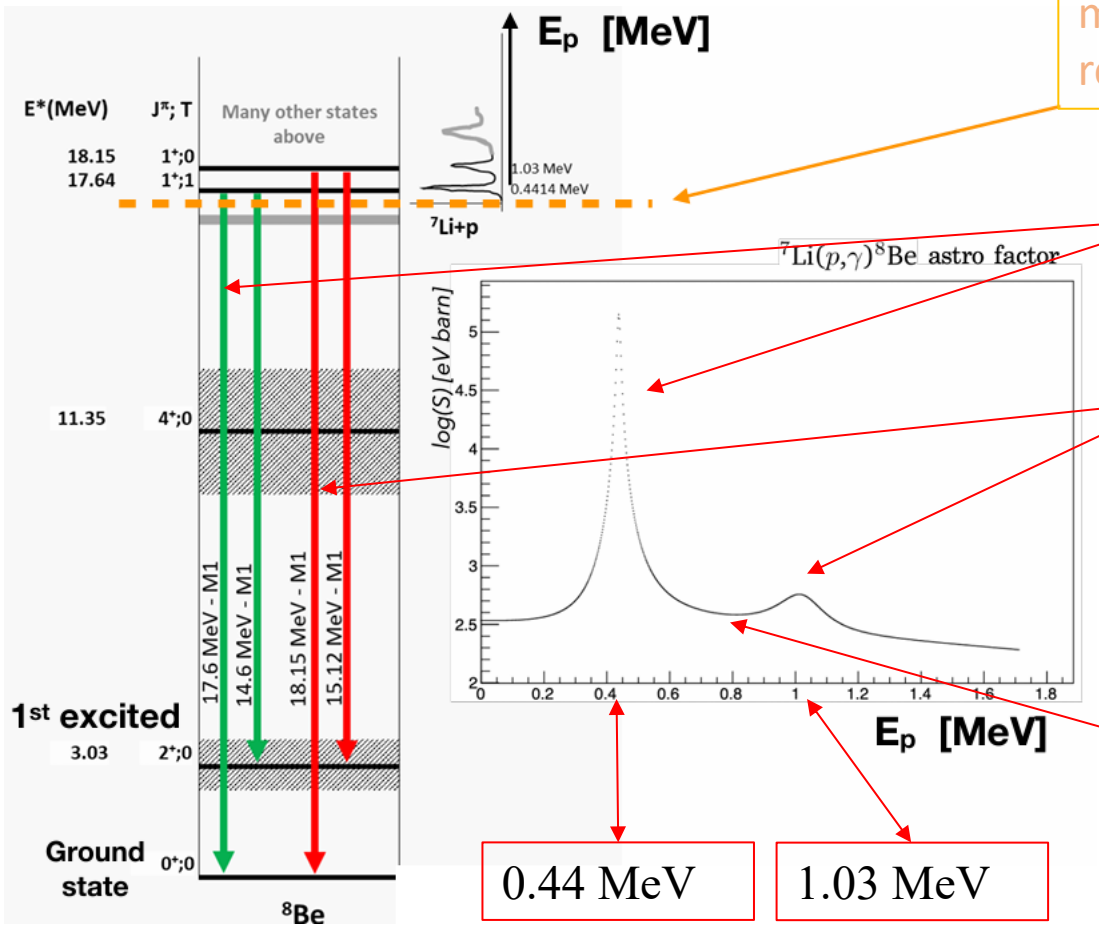


minimum energy level reached in $^7$Li + p

$^8$Be* 17.6 MeV
$J^P = 1^+$ excited state

$^8$Be* 18.1 MeV
$J^P = 1^+$ excited state

non-resonant $^7$Li proton capture forming states of energy continuously from above the 17.6 MeV state to below the 18.1 MeV state

0.44 MeV

1.03 MeV

# Reaction channels detected by MEG II

Both the **18.1 MeV excited state** (by $H^+$ , $E_p$~1.08 MeV) and the **17.6 MeV excited states** (by $H_2^+$ +, $E_p \leq 0.54$ MeV ) were formed, plus possibly a non-resonant contribution **(direct proton capture)** due to incident proton energy loss in the target before interaction

**$E_p$** ≡ proton kinetic energy

$^8$Be* 17.6 MeV $J^P = 1^+$ excited state region

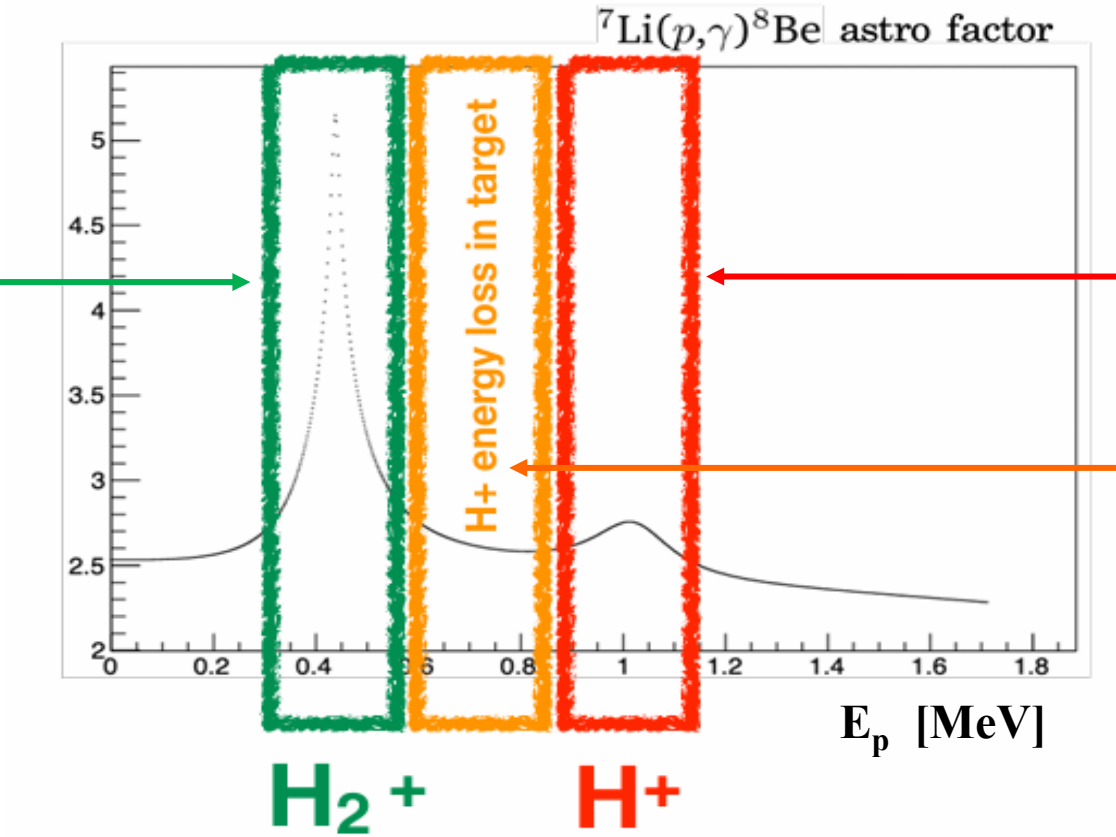


$^8$Be* 18.1 MeV $J^P = 1^+$ excited state region

non-resonant region

# Reaction channels detected by MEG II

Channels of physical interest detected in the MEGII apparatus :

$^{7}Li + p \rightarrow {}^{8}Be^{*}$ (18.1 MeV) $\rightarrow {}^{8}Be\ e^{+}e^{-}$ ($E_{ee}$ =18.1 MeV)

$^{7}Li + p \rightarrow {}^{8}Be^{*}$ (17.6 MeV) $\rightarrow {}^{8}Be\ e^{+}e^{-}$ ($E_{ee}$ =17.6 MeV)

non-interesting channels detected :

$^{7}Li + p \rightarrow {}^{8}Be^{*}$ (18.1 MeV) $\rightarrow {}^{8}Be^{*}$ (3.0 MeV) $e^{+}e^{-}$ ($E_{ee}$ =15.1 MeV)
↳ $^{8}Be\ \gamma$ (3 MeV, not detected)

$^{7}Li + p \rightarrow {}^{8}Be^{*}$ (17.6 MeV) $\rightarrow {}^{8}Be^{*}$ (3.0 MeV) $e^{+}e^{-}$ ($E_{ee}$ =14.6 MeV)
↳ $^{8}Be\ \gamma$ (3 MeV, not detected)

$^{7}Li + p \rightarrow {}^{8}Be^{*}$ (non-resonant between 17.6 and 18.1 MeV) $\rightarrow {}^{8}Be\ e^{+}e^{-}$ ($E_{ee}$ = continuum)

$^{7}Li + p \rightarrow {}^{8}Be^{*}$ (non-resonant between 17.6 and 18.1 MeV) $\rightarrow {}^{8}Be^{*}$(3.0 MeV) $e^{+}e^{-}$ ($E_{ee}$ = continuum)
↳ $^{8}Be\ \gamma$ (3 MeV, not detected)

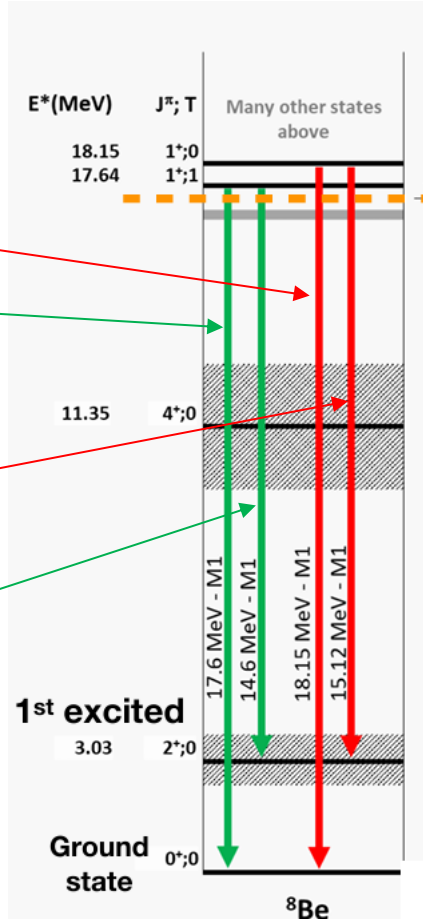

# The MEG II apparatus for the $^{7}Li + p \rightarrow {}^{8}Be$ X17 search, cont.d

## Target

7 μm LiPON Lithium Phosphorous Oxynitride ($Li_{3-x}PO_{4-y}N_{x+y}$) target on 25 μm Cu substrate.

LiPON preferred over $Li_2O$ (more stable chemically).

LiPON preferred over LiF : the 6 MeV fluorine line produces too many γ converting in $e^+e^-$ in the apparatus with an overwhelming background

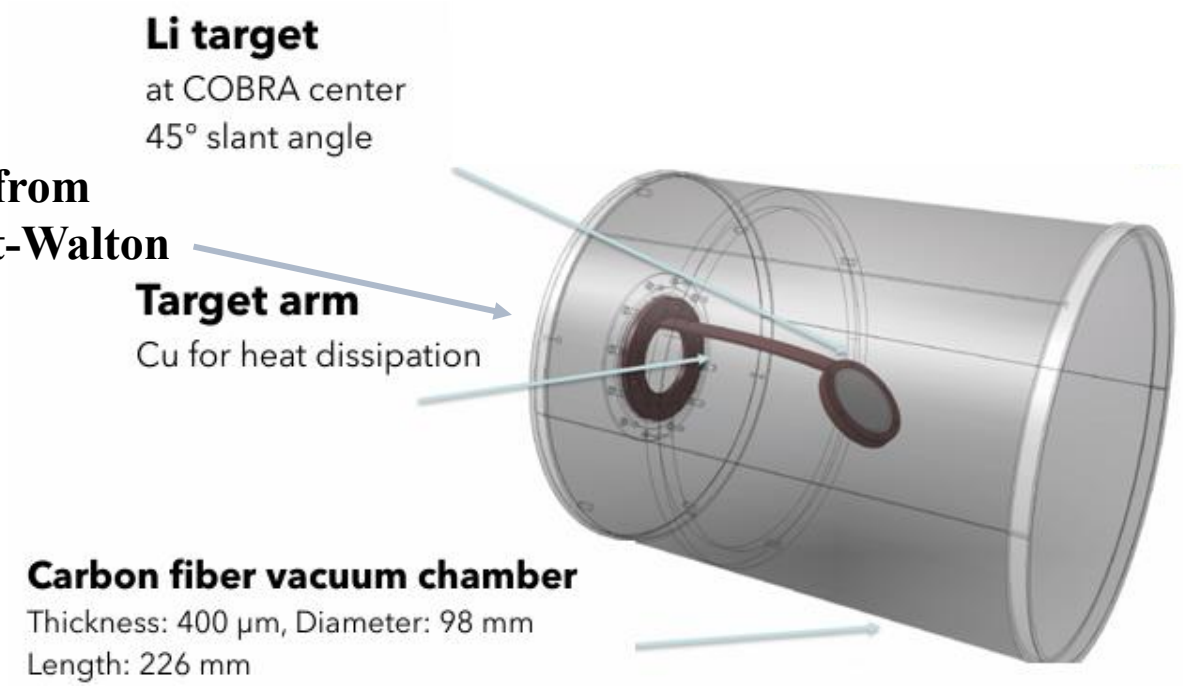


target
irregular surface.

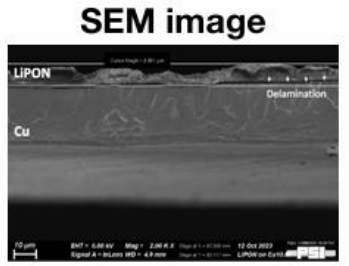


target

# The MEG II apparatus for the $^7Li + p \rightarrow {}^8Be$ X17 search, cont.d

## $e^+ e^-$ tracking and timing devices

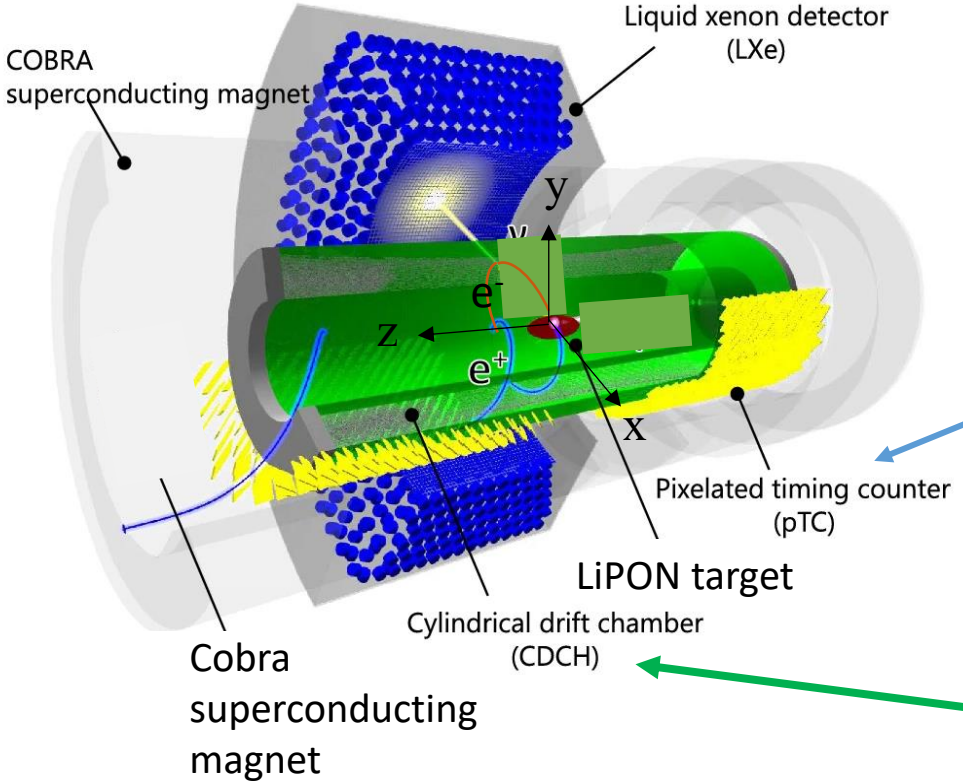


**pTC** : 512 plastic tiles, 35 ps resolution on the positron or electron track time of passage

- single volume : He-isobutane-isopropyl alchol-$O_2$
- 9 concentric layers of 192 cells each
- momentum resolution : 90 keV at $E_e \sim 52$ MeV

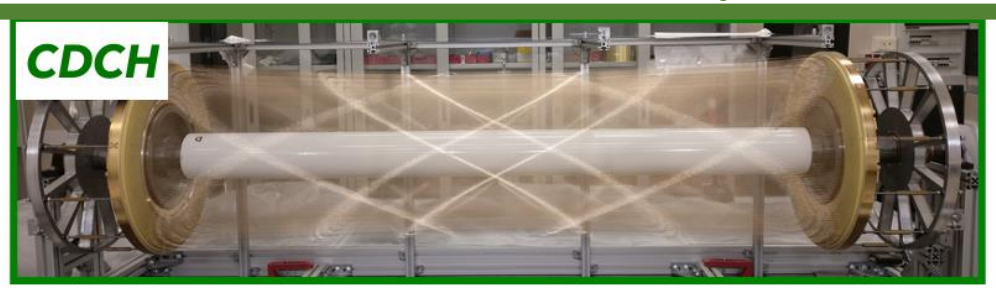

# The MEG II apparatus for the $^{7}Li + p \rightarrow {}^{8}Be$ X17 search

## γ detectors

Used for monitoring, background checks and signal normalization

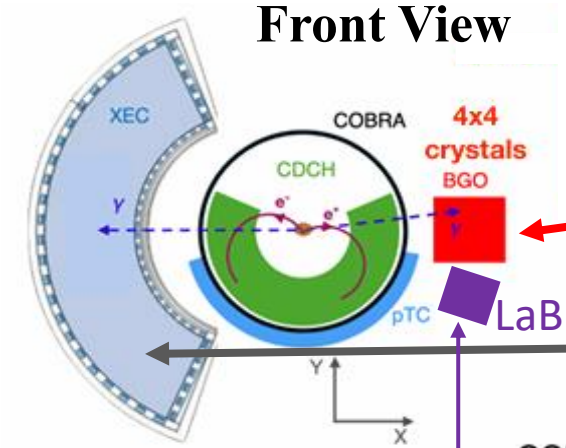



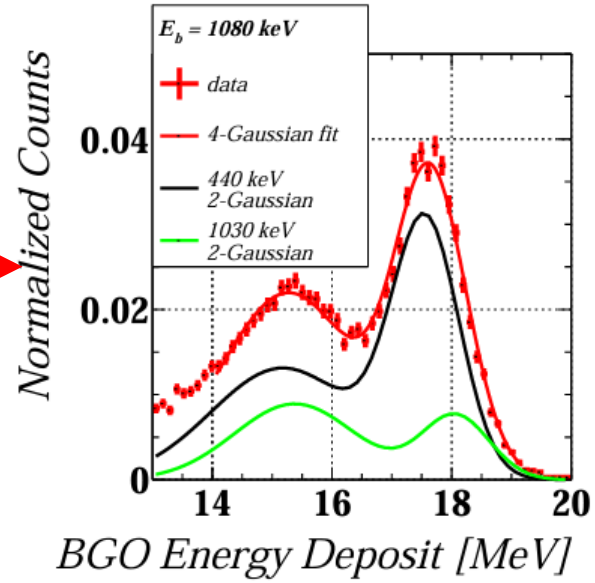


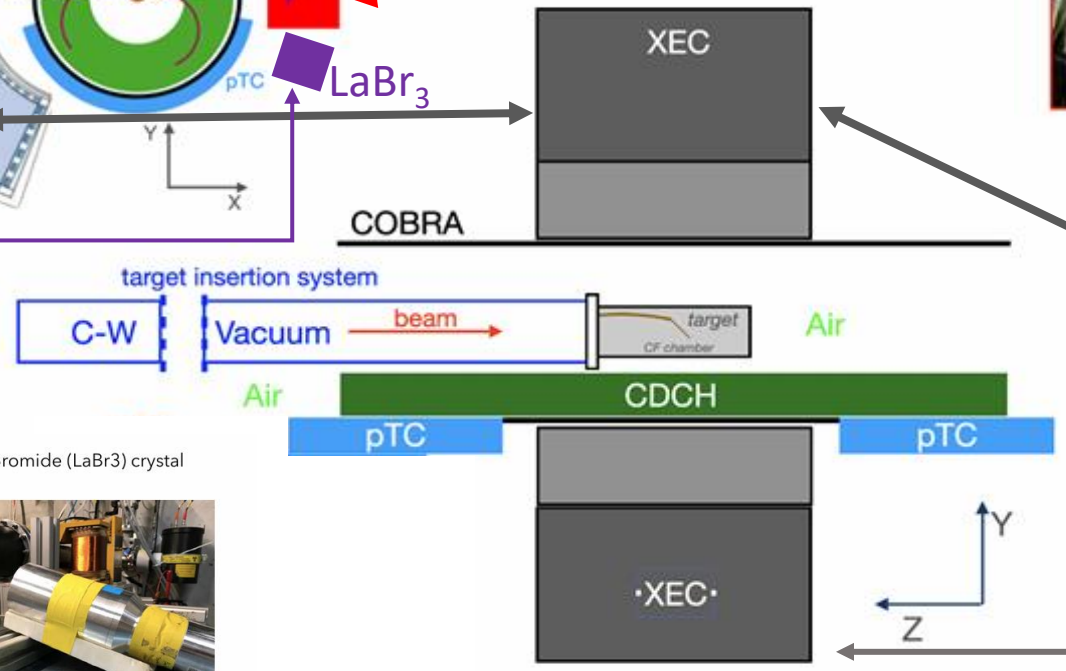


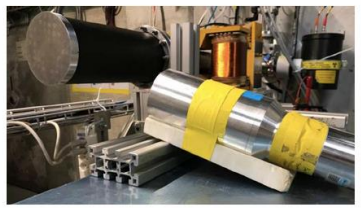

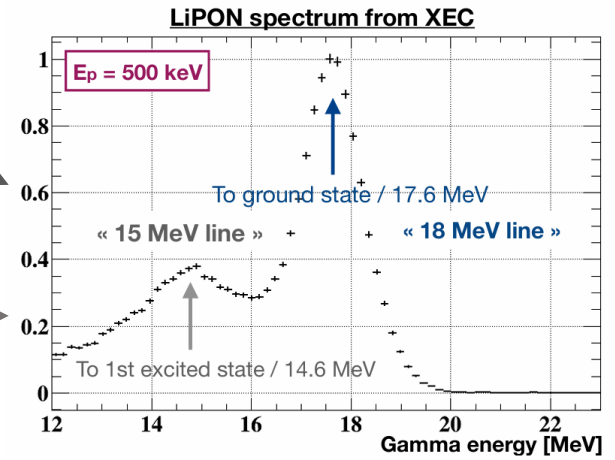

# Montecarlo for the X17 signal

The very detailed MonteCarlo used to simulate the MEG II apparatus in the $\mu^+ \rightarrow e^+\gamma$ search is used also for the X17 search, with the obvious changes regarding the target and the material sorrounding it.

The X17 boson is assumed to decay to $e^+ e^-$ isotropically in its c.m.s.

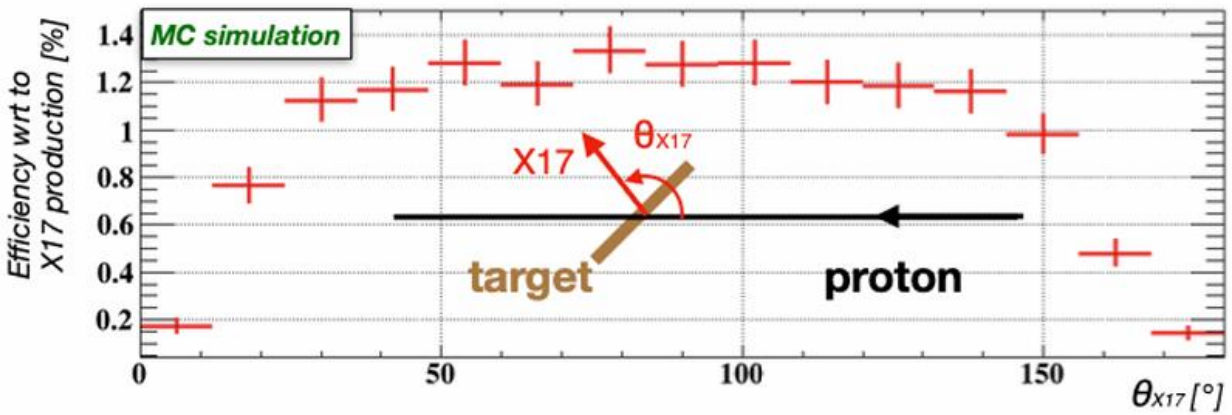


Average opening angle between $e^+$ and $e^-$ expected depending on the X17 boson mass

**The apparatus acceptance covers a large angle of emission of a X17 boson (ATOMKI acceptance is only around 90°)**

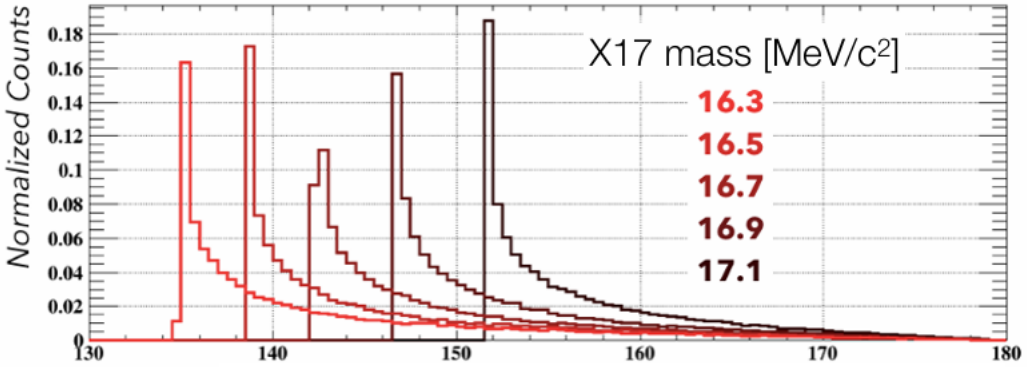

# Montecarlo simulation of the $e^+e^-$ backgrounds

Physics backgrounds : IPC and EPC

**IPC** : the **Zhang-Miller model** was used because it allows for interference between the resonant and the non-resonant continuum contributions with different multipole character

this choice is confirmed to be good also
by a fit to the ATOMKI
$^7\mathrm{Li} + \mathrm{p} \rightarrow {}^8\mathrm{Be}\ e^+e^-$ IPC background

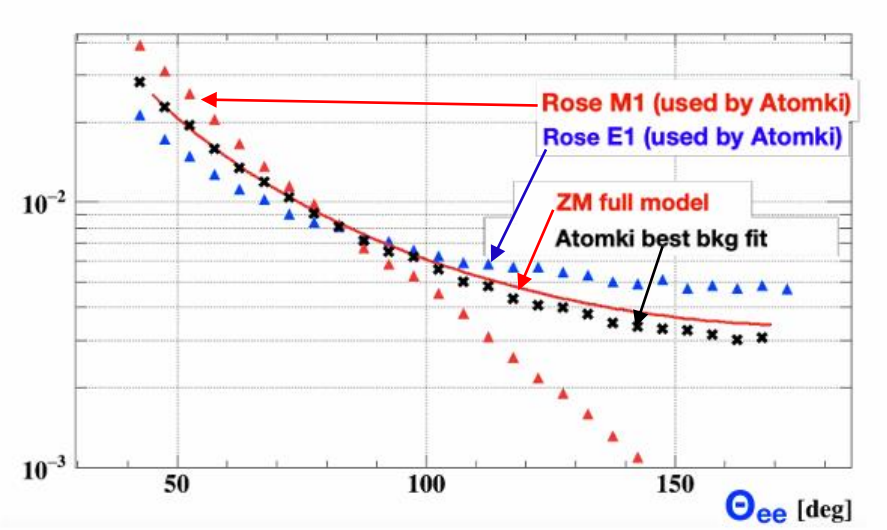


**EPC** : γ converting in the apparatus material. Simulated with GEANT4

**Compton electrons** contributing to fake track pairs : simulated with GEANT4

# Montecarlo simulation of the $e^+e^-$ backgrounds

Detailed simulation of the **EPC** background produced by γ interacting mainly in the target support ring made of copper

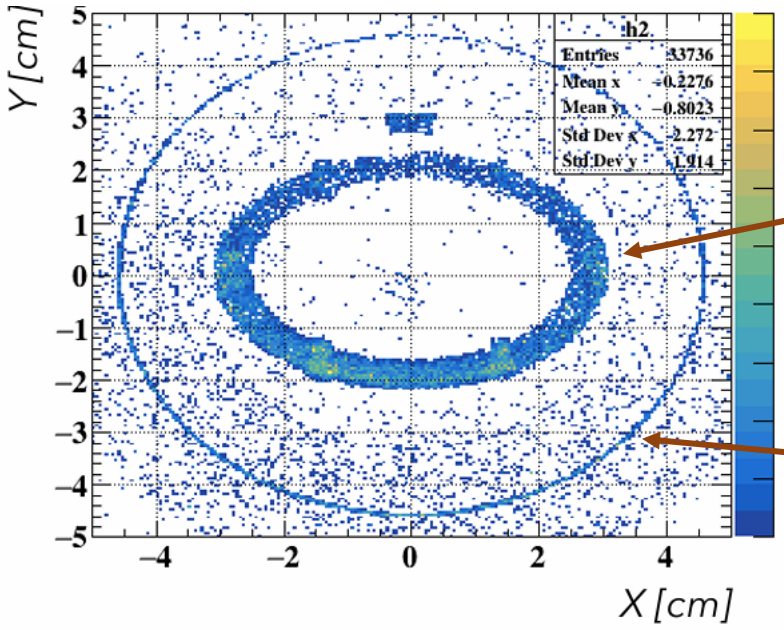


front view

target and Cu
target holder

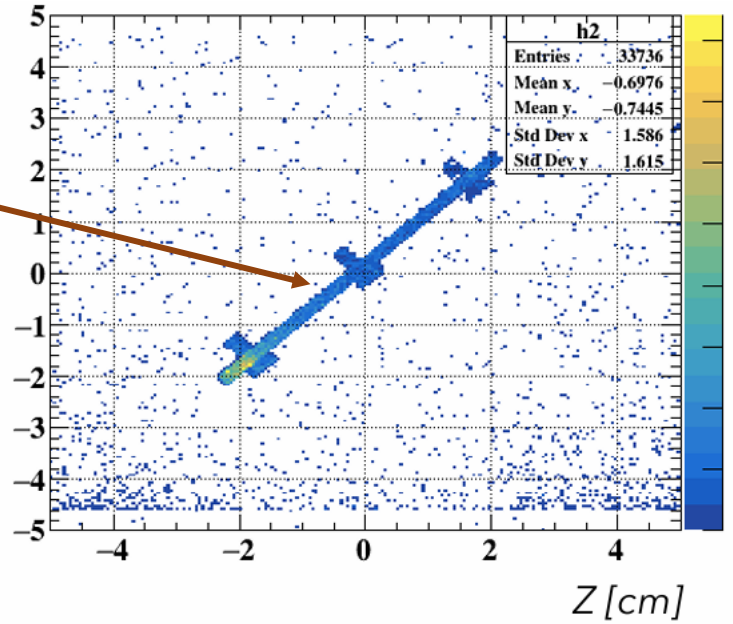


side view

# Montecarlo simulation of the $e^+e^-$ backgrounds

Physics backgrounds : IPC and EPC

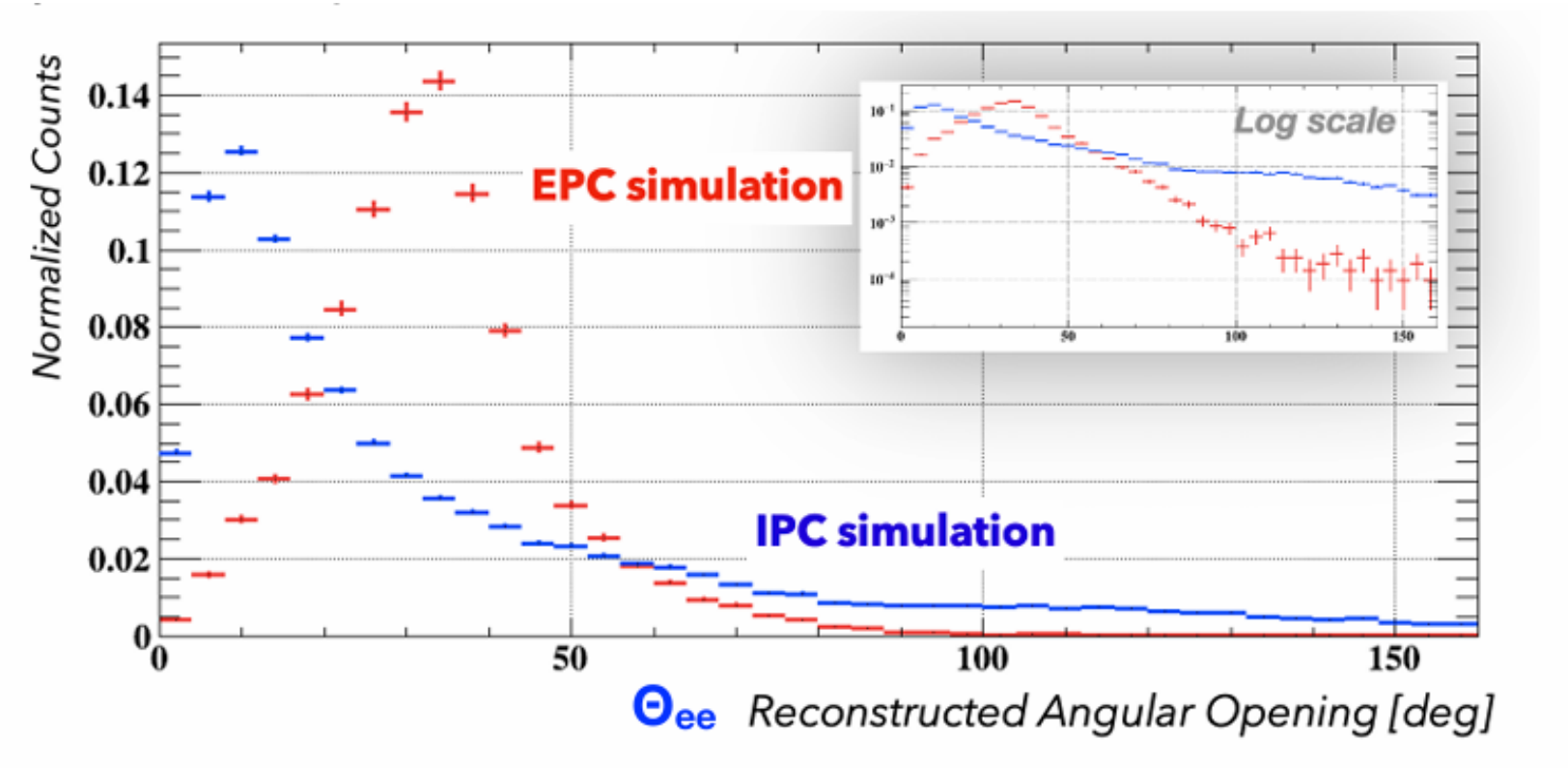


IPC 100 times larger than EPC in the signal region ( $\Theta_{e^+e^-} \sim 140°$ )

# Trigger strategy

With the aid of the MC a good trigger strategy was identified

No online track reconstruction, and no CDCH hit wire number information available.
Trigger based on waveform CDCH amplitude and on number of hits in CDCH and pTC

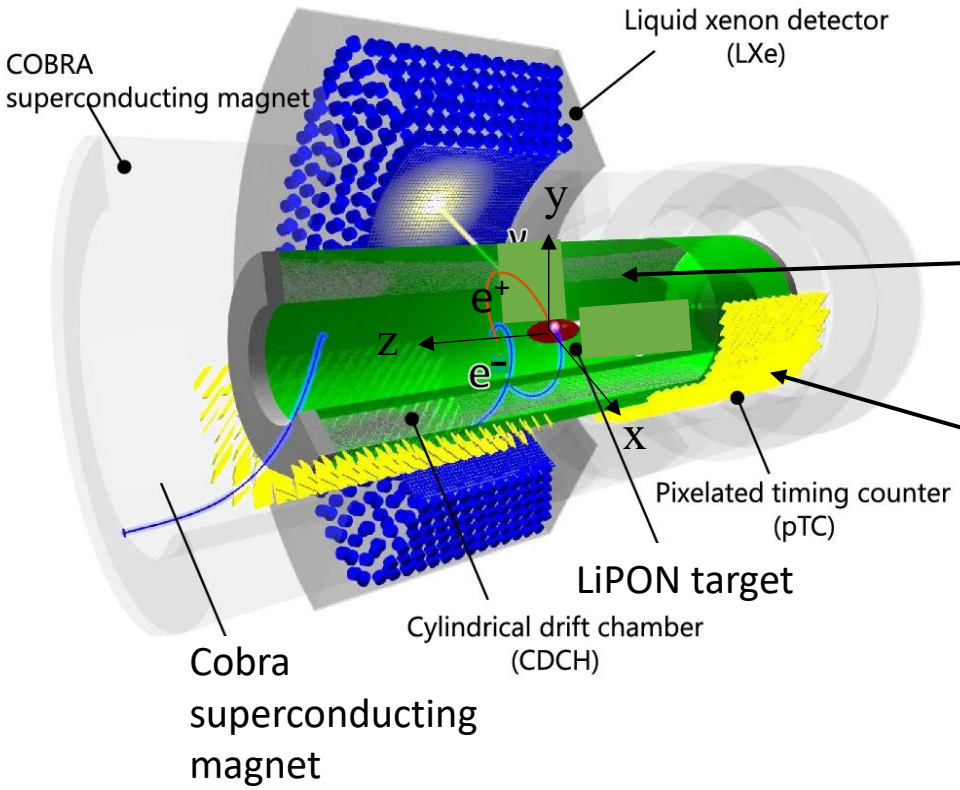


**Trigger**

18 hits in the CDCH (it tends to select real tracks produced at the target center and favours the presence of pairs) with pulse height > 60 mV (it tends to eliminate noise hits)

a hit in the pTCounter (it assures the presence of at least one particle with energy ≥ 6 MeV )

# Trigger strategy

**Trigger**

- 18 hits in the CDCH with pulse height > 60 mV
- a hit in the pTCounter

**16 % trigger efficiency for the X17 signal**

Montecarlo

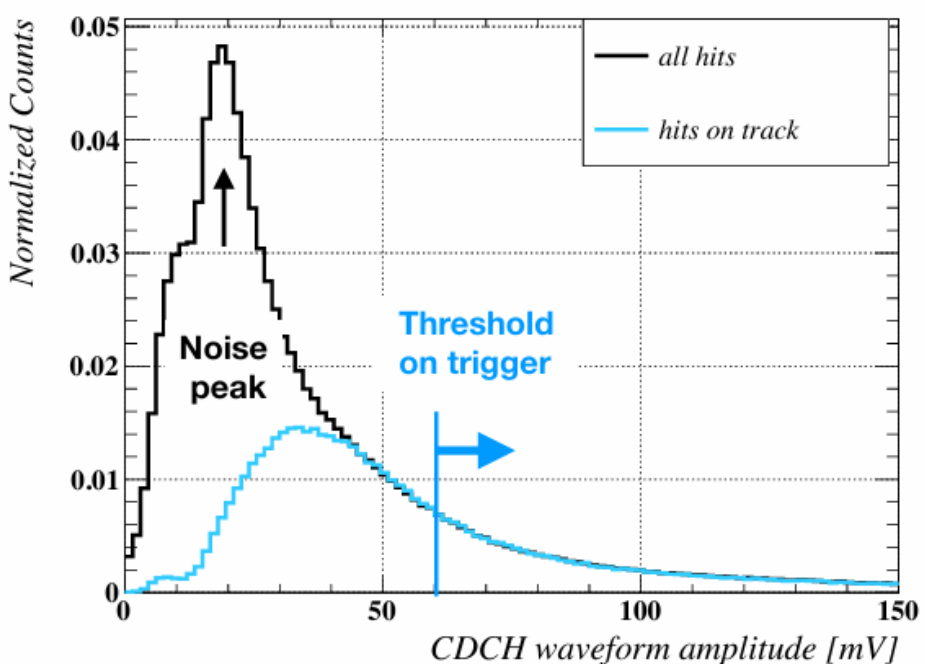


60 mV threshold tends to eliminate noise hits)

Montecarlo

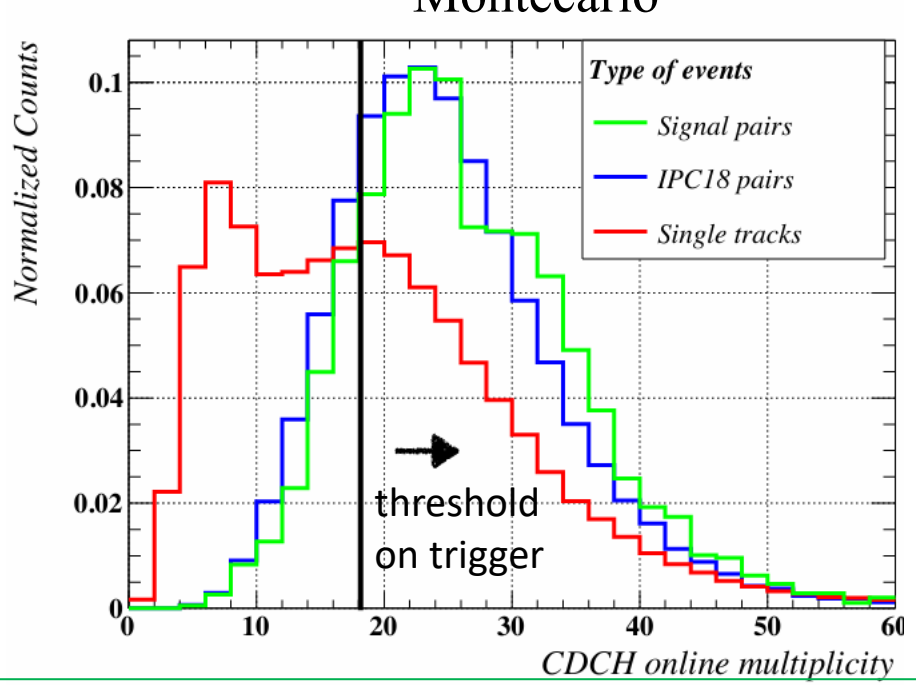


18 hits tend to select real tracks produced at the target center and favours the presence of pairs

# The Data Taking

**Test run in 2022** : proton beam tuning, LiF (later discarded) and LiPON target tests, trigger settings optimization, reconstruction algorithms optimization

**Physics run in 2023** :

- 4 weeks with proton beam energy at 1080 KeV, 10 μA current intensity

- beam composition **:** ~ 75% $H^+$ and ~ 25% $H_2^+$ → possibility to form both the 18.1 MeV and the 17.6 MeV $^8Be^*$ excited states

- Thickness LiPON target ~ 7 μm
- ~ 75 M events collected

- ~ 300 k events with $e^+e^-$ pairs selected

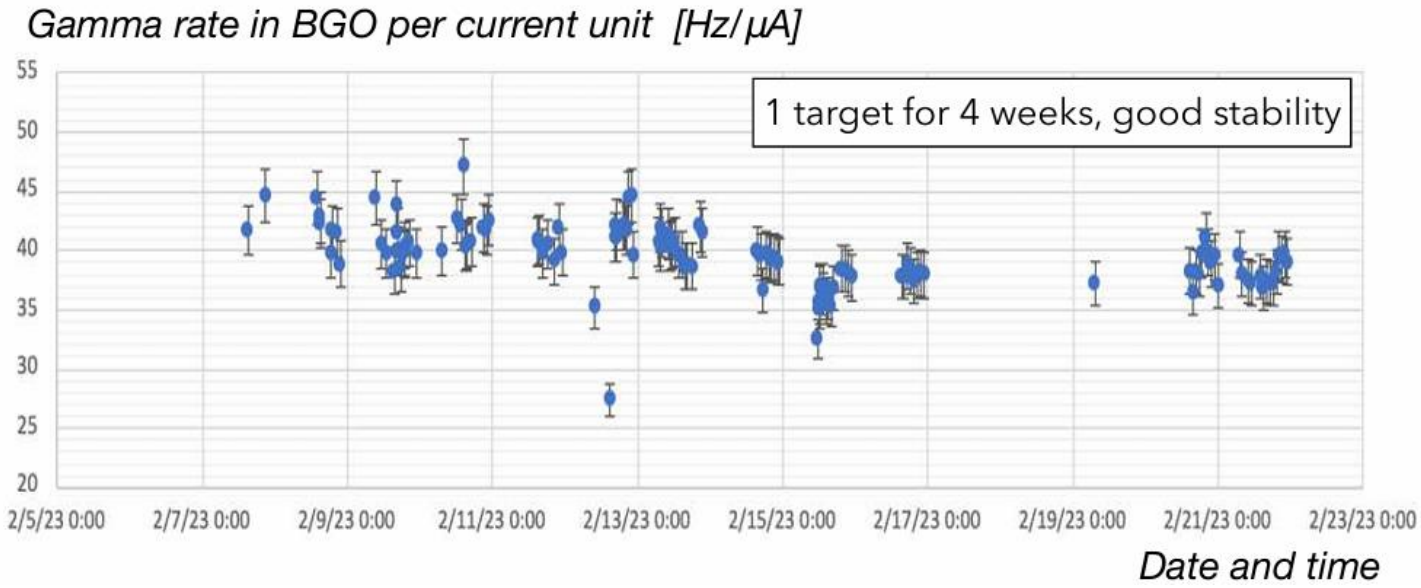

# $e^+ e^-$ reconstruction in MEG-X17 apparatus

## An event with a good pair of tracks

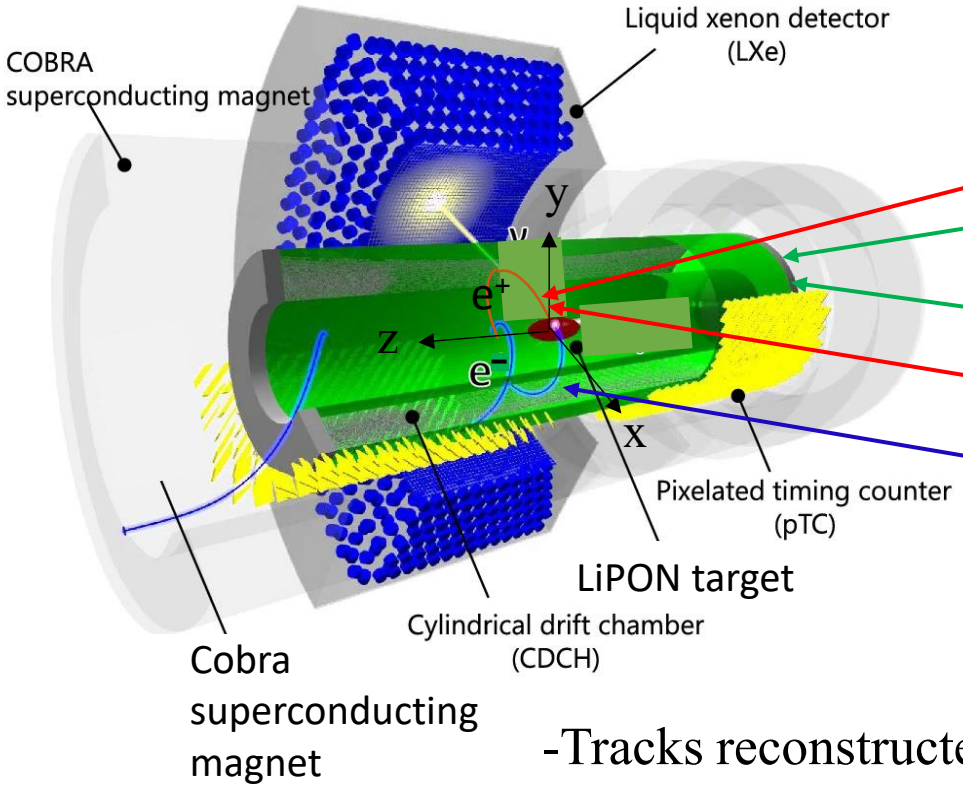


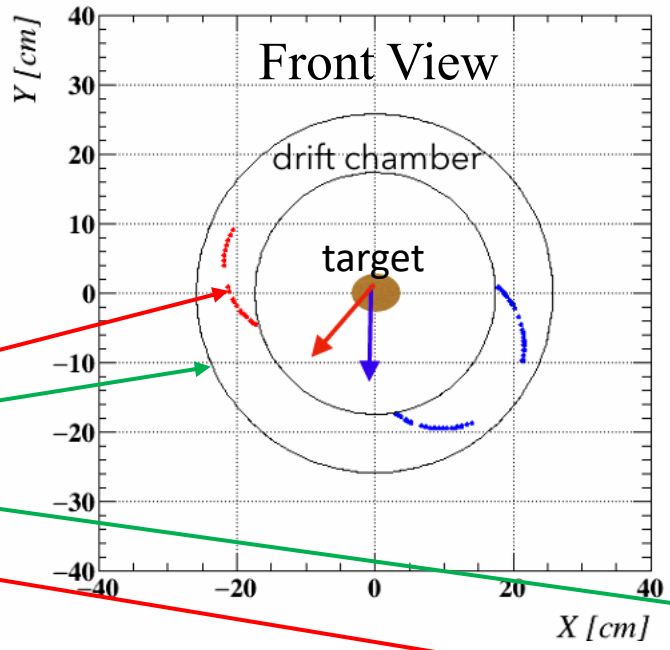


negative track

positive track

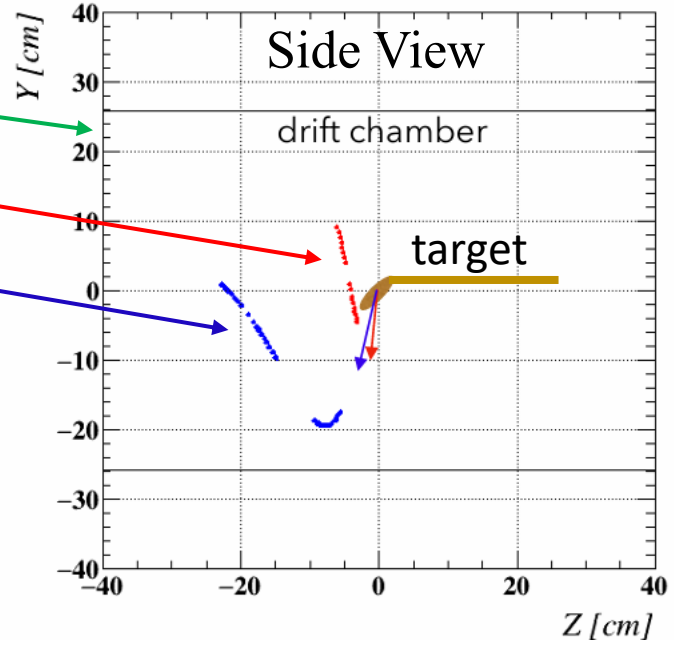


-Tracks reconstructed with a Kalman Filter based pattern recognition and track fitting

- good track : at least 10 hits in Drift Chamber

# $e^+ e^-$ reconstruction in MEG-X17 apparatus

**An event with a fake pair of tracks**

Front View

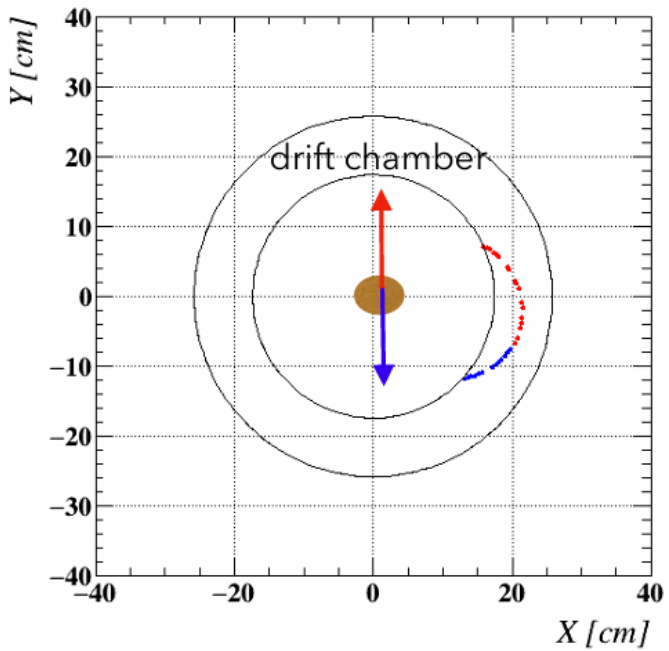


Side View

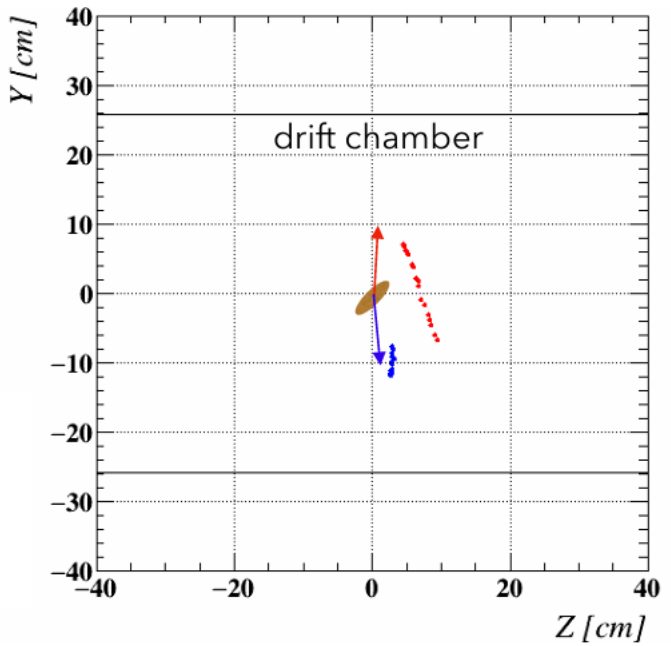


two pieces of one track are reconstructed as two tracks back-to-back , $\Theta_{ee} \sim 180°$

# Rejecting the fake $e^+e^-$ pairs

Fake tracks are : a) short

b) if long they hits are less dense → consecutive hits are more spaced

c) emitted orthogonally to the beam with the first hit Z position close to 0

**Fake rejection cuts were developed, their effectivenes was checked against Montecarlo simulations**

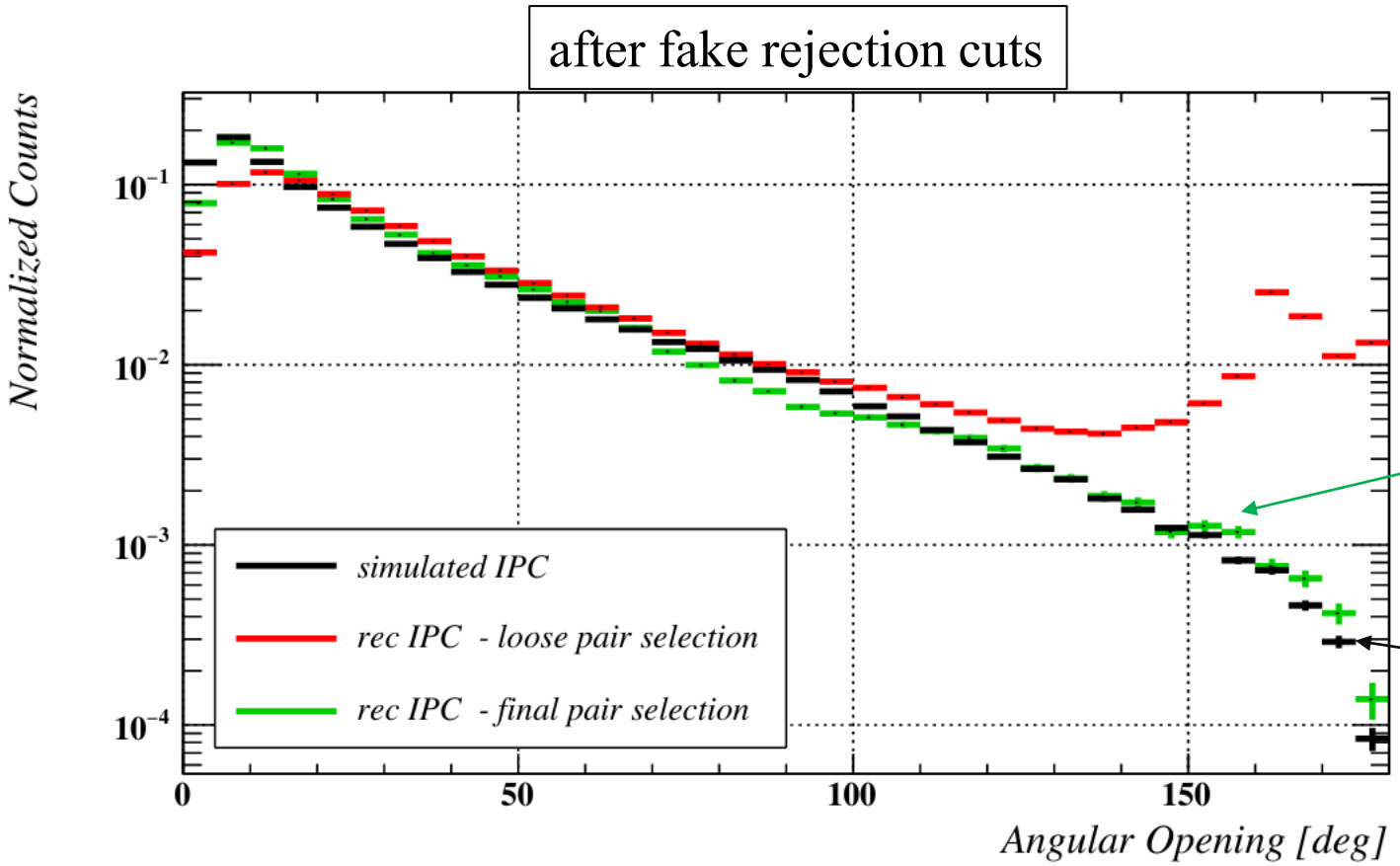


experimental data
$e^+e^-$ angular distribution
after fake rejection cuts

MC simulation data
$e^+e^-$ angular distribution

# Selection of the $e^+e^-$ signal, details

$z_{vtx} \equiv z$ of track at Point Of Closest Approach (POCA) to the beam axis
$z_b \equiv z$ position of the beam spot center at target

track must go away from the target
$z_f$ , $z_l \equiv z$ position of first/last hit;

$\mu_{hit} \equiv$ hit density along the track trajectory

std $\equiv \sigma$ of distribution of distances of contiguous hits of a given track; real tracks don't have large $\sigma$

$z_{mean} \equiv$ mean z of track hits; $\theta \equiv$ polar angle of track momentum at vertex ; this cut requires the consistency between the direction along z and the sign of the hits z-position

| Selection | |
|---|---|
| $n_{hits} \geq 10$ | n. hits in a track |
| $\lvert z_{vtx} - z_b \rvert \leq 2.5$ cm | |
| $T_{0l} - T_{0f} \geq 0$ | $T_{0l} \equiv$ time of the last hit of a track ; $T_{0f} \equiv$ time of the first hit |
| $(z_l - z_f) \times sgn(z_f) \geq 0$ | |
| propagation length $\geq 35$ cm | distance travelled by a track from POCA to first chamber hit |
| if $10 \leq n_{hits} \leq 16$, $\mu_{hit} \geq 1.1$ hits/cm | |
| *if* $\mu_{hit} > n_{hits}/12 - 2/3$: $\mu_{hit} \geq 0.8$ hits/cm, track score $\geq 20$ | track score $\equiv 10\ \mu_{hit} + n_{hits}$; cut inferred from montecarlo |
| Consecutive hits distance std $< 0.9$ cm | |
| $\lvert z_f \rvert \geq 2.5$ cm | $z_f \equiv z$ position of the first hit; the cut excludes tracks emitted orthogonal to the beam direction for which it is difficult to decide the sign of the charge |
| $z_{mean} \times (\theta - 90°) < 0$ | |
| No hits in common between $e^+$ and $e^-$ tracks | |
| $e^+e^-$ vertices distance $< 3$ cm | |

# The $e^+e^-$ signal, resolution and efficiencies

**….from MonteCarlo**

| | X17<br>16.9 MeV/$c^2$ | IPC<br>18 MeV | EPC<br>18 MeV |
|---|---|---|---|
| trigger selection eff. | 16% | 4.7% | 0.026% |
| $e^+$ selection eff. (wrt trg) | 24% | 26% | 13% |
| $e^+e^-$ selection eff. (wrt trg) | 2.5% | 2.3% | 0.6% |
| $\Theta_{ee}$ resolution [deg] | $5.6 \pm 0.2$ | $5.5 \pm 0.1$ | // |
| $E_{sum}$ resolution [MeV] | $0.58 \pm 0.02$ | $0.69 \pm 0.01$ | // |

# Analysis strategy of the $e^+e^-$ signal

**Two variables chosen (the same as ATOMKI) for a 2-D plot analysis**

$\mathbf{E_{sum}} \equiv E(e^+) + E(e^-)$

$\mathbf{\Theta_{ee}} \equiv$ opening angle between $e^+$ and $e^-$

(avoid the use of Mass($e^+e^-$) and $\Theta_{ee}$ because Mass depends on $\Theta_{ee}$ and consequently they are correlated)

if a signal like in ATOMKI were present one would expect an excess of data points at $E_{sum} \sim 17$ MeV and $\Theta_{ee} \sim 140°$

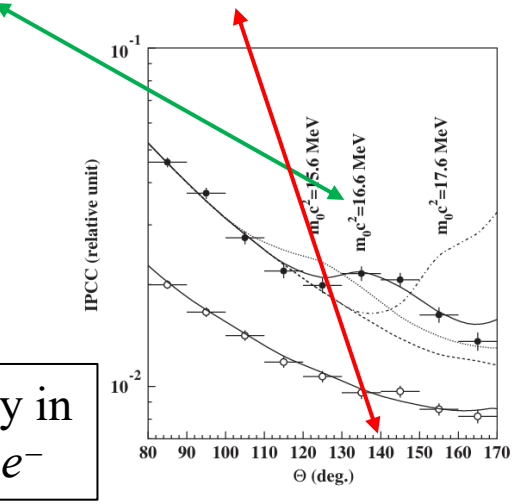


ATOMKI anomaly in $^7Li + p \rightarrow {}^8Be\ e^+e^-$

# Analysis strategy of the $e^+e^-$ signal

Define a **'BLIND BOX'** where the signal is supposed to be :

$$16 < E_{sum} < 20 \text{ MeV}$$
$$115° < \Theta_{ee} < 160°$$

**Validate the background distributions** with fits in the sideband regions before opening the box

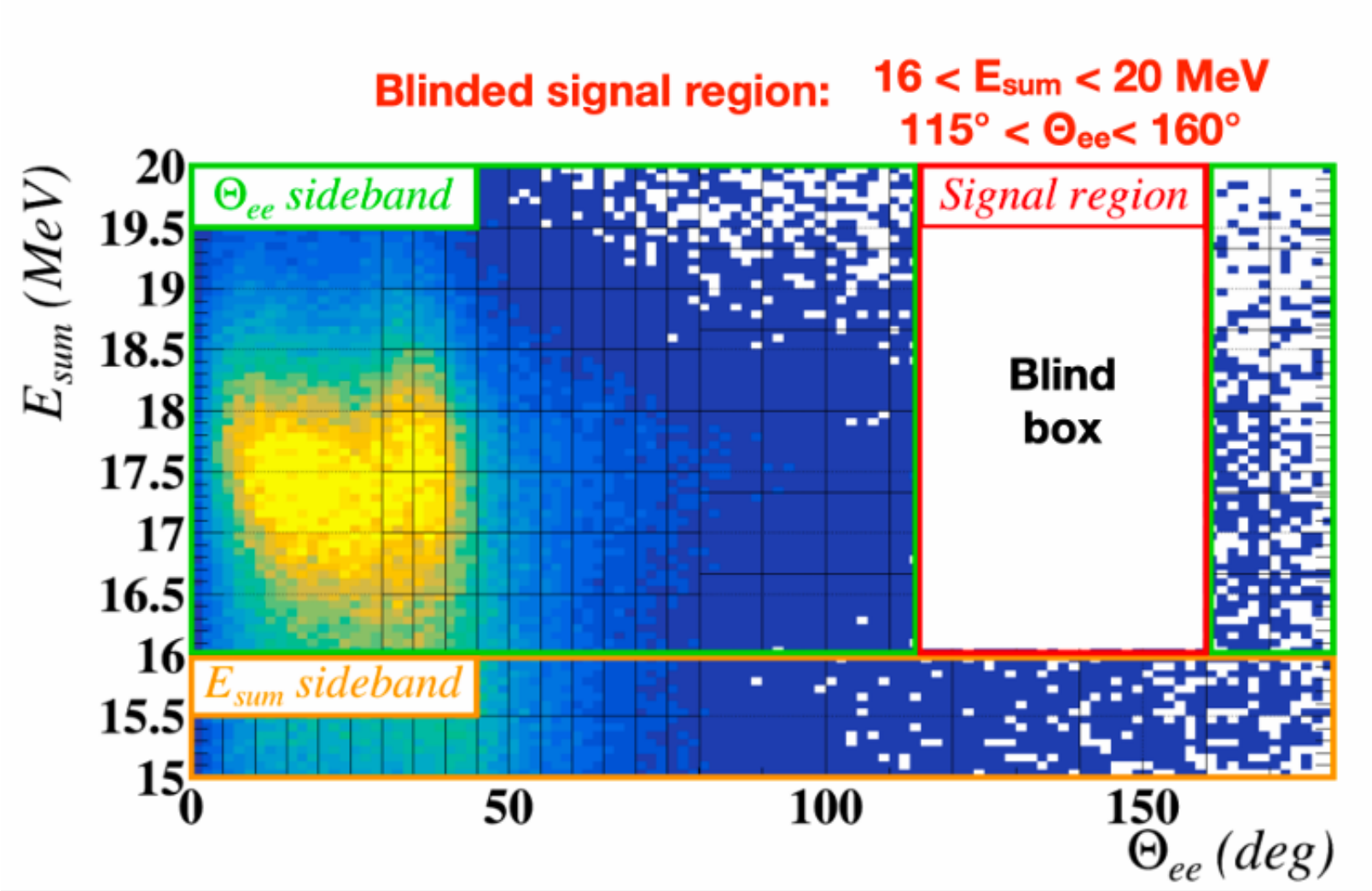

# Fit to the 2-D histogram, composition of the total PDF

The two dimensional histogram was fitted with a **binned likelihood distribution**.

The total Probability Distribution Functions was the sum of :

**$e^+e^-$ signal distribution from the X17**

two distributions : one for X17 produced by the 18.1 MeV Be* resonance
one for X17 produced by the 17.6 MeV Be* resonance

**$e^+e^-$ physics background distributions :**

six $e^+e^-$ IPC physics processes :

two $e^+e^-$ EPC processes

**$e^+e^-$ non-physical background distribution :**

fake $e^+e^-$ pairs from random track combinations

# Fit to the 2-D histogram, X17 signal PDF

**The X17 was assumed to decay to $e^+e^-$ isotropically in its cms**

The $E_{sum}$ - $\Theta_{ee}$ distribution depends on $\mathbf{E_{X17}}$ in the lab system and the **X17 mass ($\equiv \mathbf{M_{X17}}$)**

Two sets of distributions were generated by the Montecarlo

1) a set of X17 produced by the 18.1 MeV $^8$Be* resonance $\rightarrow$ $\mathbf{E_{X17} = E_{sum} = 18.1}$ **Mev** in lab system **(this is the ATOMKI hypothesis)**

2) a set of X17 produced by the 17.6 MeV $^8$Be* resonance $\rightarrow$ $\mathbf{E_{X17} = E_{sum} = 17.6}$ **Mev** in lab system

Each distribution ($\equiv$ template) of a set was generated for a value of $M_{X17}$ : 6 different $M_{X17}$ values in total, spanning uniformly the physical region of interest, **from 16.3 MeV/$c^2$ to 17.3 MeV/$c^2$** .

The generated events then passed through the detailed detector response simulation.

# Fit to the 2-D histogram, X17 signal PDF

$M_{X17}$ was a parameter of the fit and so it varied continuously. The $E_{sum}$ - $\Theta_{ee}$ distribution for **any** value of $M_{X17}$ between 16.3 MeV/$c^2$ and 17.3 MeV/$c^2$ was obtained with a histogram **interpolation** technique of the templates performed on a bin-by-bin basis (vertical morphing[1])

[1] M.Baak *et al.*, NIM A 771, 39 (2015)

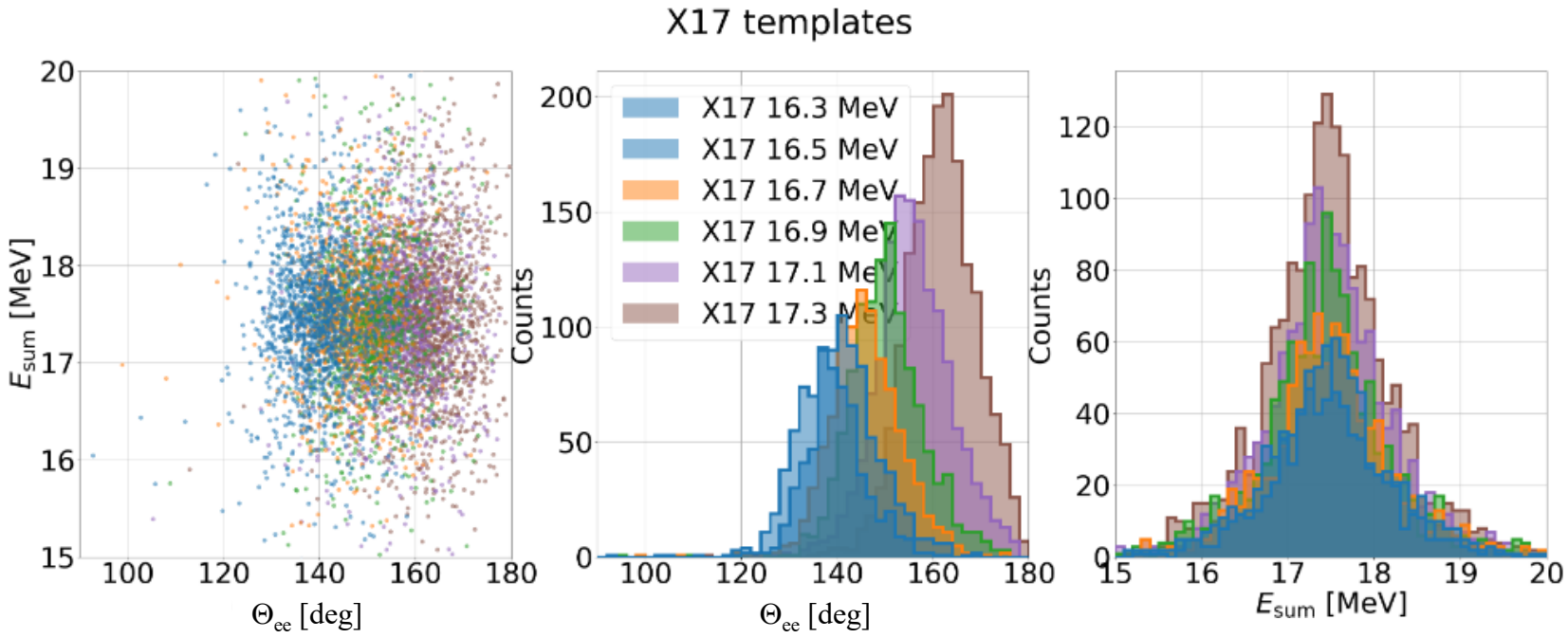


the template distributions $E_{sum}$ - $\Theta_{ee}$ generated for 6 different values of $M_{X17}$ and used in the histogram interpolation (morphing)

# Fit to the 2-D histogram, physics background PDF's

## Six $e^+e^-$ IPC physics processes :

$^7Li + p \rightarrow {}^8Be^*$ (18.1 MeV) $\rightarrow$ **$^8Be$ $e^+e^-$ ($E_{ee}$ =18.1 MeV)**

$^7Li + p \rightarrow {}^8Be^*$ (18.1 MeV) $\rightarrow$ **$^8Be^*$ (3.0 MeV) $e^+e^-$ ($E_{ee}$ =15.1 MeV)**

$^7Li + p \rightarrow {}^8Be^*$ (17.6 MeV) $\rightarrow$ **$^8Be$ $e^+e^-$ ($E_{ee}$ =17.6 MeV)**

$^7Li + p \rightarrow {}^8Be^*$ (17.6 MeV) $\rightarrow$ **$^8Be^*$ (3.0 MeV) $e^+e^-$ ($E_{ee}$ =14.6 MeV)**

$^7Li + p \rightarrow \rightarrow {}^8Be^*$ non resonant, energy between **17.6 and 18.1 MeV**
$\rightarrow$ **$^8Be$ $e^+e^-$ ($17.6 < E_{ee} < 18.1$ MeV )**

$^7Li + p \rightarrow \rightarrow {}^8Be^*$ non resonant, energy chosen between **17.6 and 18.1 MeV**
$\rightarrow$ **$^8Be$ *(3.0 MeV) $e^+e^-$ ($14.6 < E_{ee} < 15.1$ MeV )**

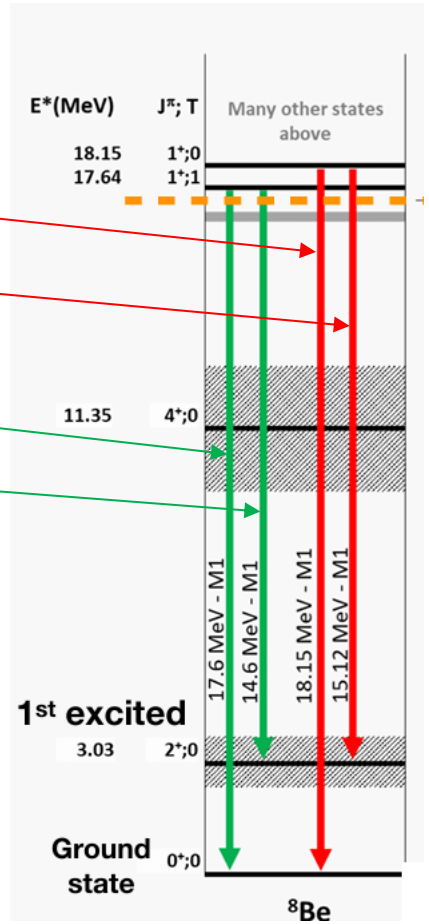


Distributions obtained by a montecarlo with a **generator according to the Zhang-Miller model** and a detailed detector response simulation

# Fit to the 2-D histogram, physics background PDF's

**Two $e^+e^-$ EPC processes, simulated with GEANT4 :**

$^7Li + p \rightarrow {}^8Be^*$ (18.1 MeV) $\rightarrow {}^8Be$ **$\gamma$ (18.1 MeV)** with the $\gamma$ converting into $e^+e^-$ in the material of the apparatus

$^7Li + p \rightarrow {}^8Be^*$ (18.1 MeV) $\rightarrow {}^8Be^*$ (3.0 MeV) **$\gamma$ (15.1 MeV)** with the $\gamma$ converting into $e^+e^-$ in the material of the apparatus

According to GEANT4 simulations no difference can be resolved in the distributions of converting $\gamma$ at similar energies (i.e. 18.1 MeV and 17.6 MeV or 15.1 MeV and 14.6 MeV)

**That's why only 18.1 and 15.1 MeV were chosen as 'representative' distributions**

# Fit to the 2-D histogram, non-physical background PDF's

**Fake pairs originated by a positive and a negative random tracks making a vertex**

Distribution obtained by combining an electron of an event with a positron of a different event and passing this pseudo-vertex through the analysis selection chain.

# Analysis strategy of the $e^+e^-$ signal

From definition of fit region it was excluded :

$16 < E_{sum} < 20$ MeV and $\Theta_{ee} < 30°$
OR
$\Theta_{ee} < 50°$ and $\Theta_{X17} < 80$

$\Theta_{X17} \equiv$ angle of emission of the $e^+e^-$ pair

because the MC could not reproduce accurately the background which was very sensitive to the beam position and to fraction of $H_2^+$

**Excluded region was anyway far from the physical region of interest**

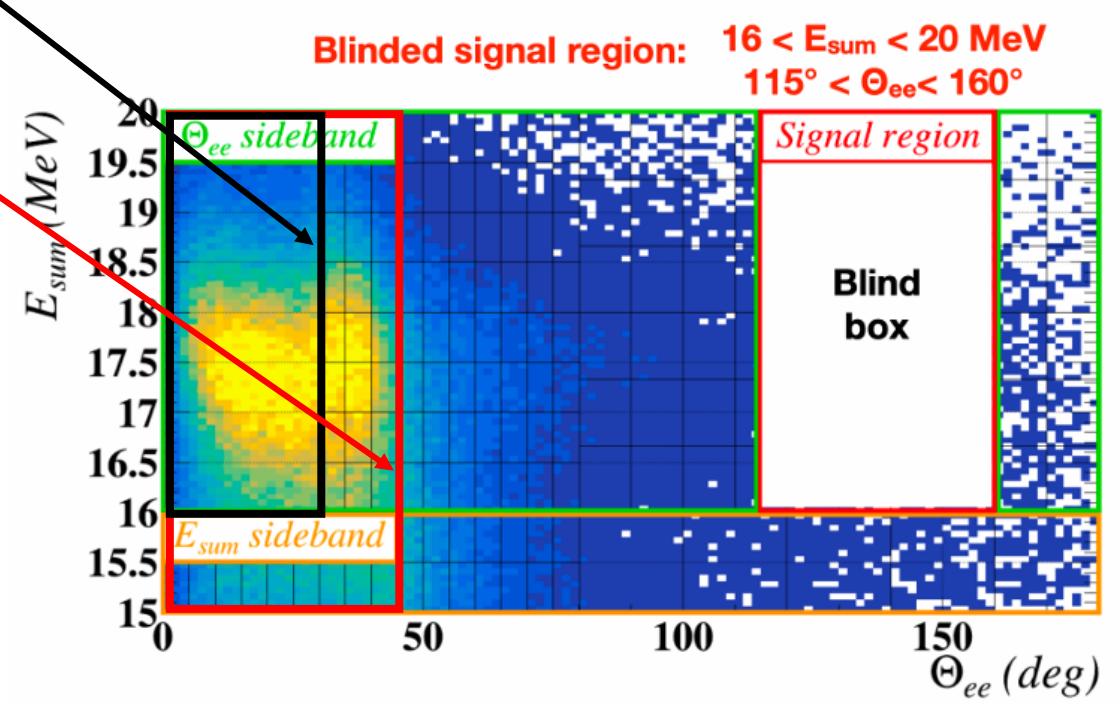

# Analysis strategy of the $e^+e^-$ signal

**All the distributions of the backgrounds were validated with fits in the sideband regions before opening the box**

Example of sideband fit

IPC 17.6 ≡ IPC 17.6 MeV + IPC 14.6 MeV

IPC 18.1 ≡ IPC 18.1 MeV + IPC 15.1 MeV

2D fit projected on the $\Theta_{ee}$ axis

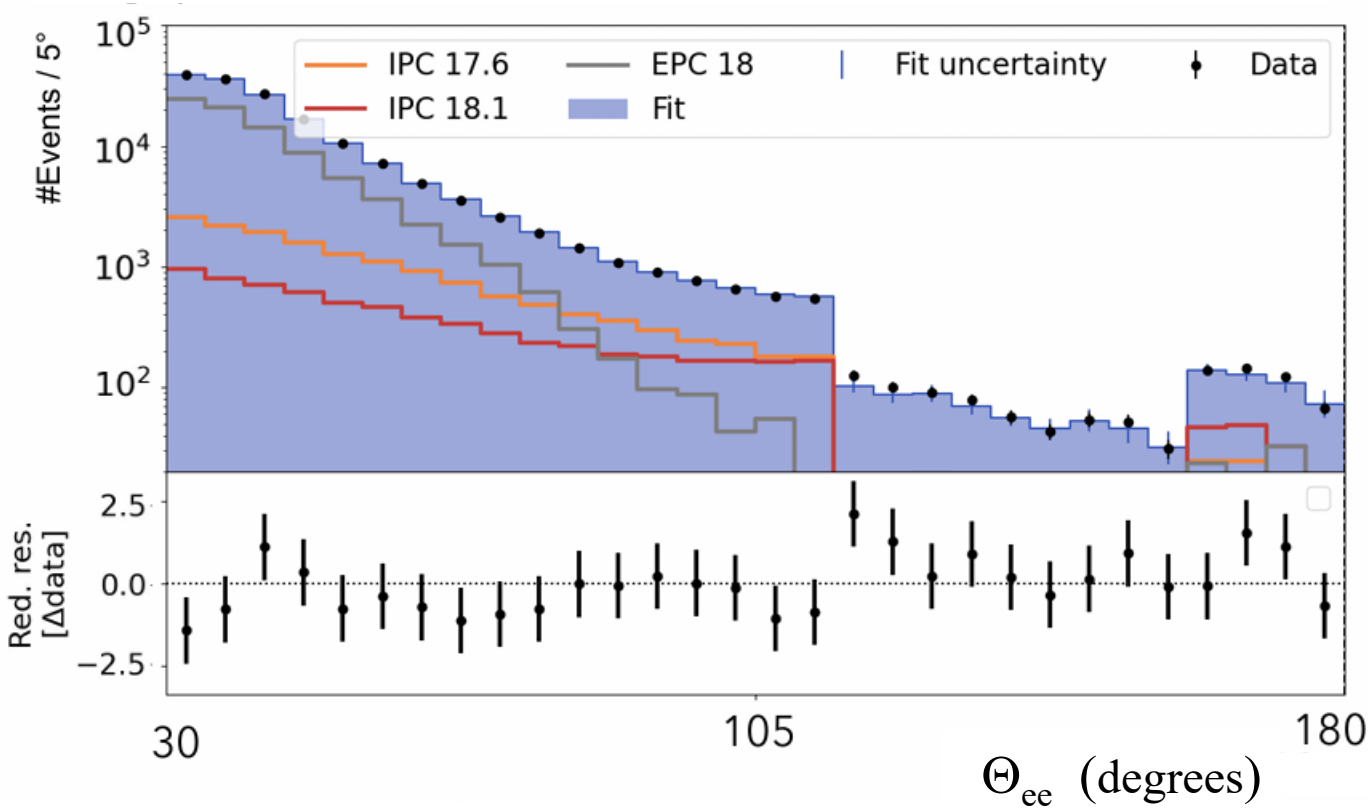

# Analysis strategy of the $e^+e^-$ signal

**All the distributions of the backgrounds were validate with fits in the sideband regions before opening the box**

A more detailed example of sideband fit. Projections on the $\Theta_{ee}$ axis of slices of $E_{sum}$

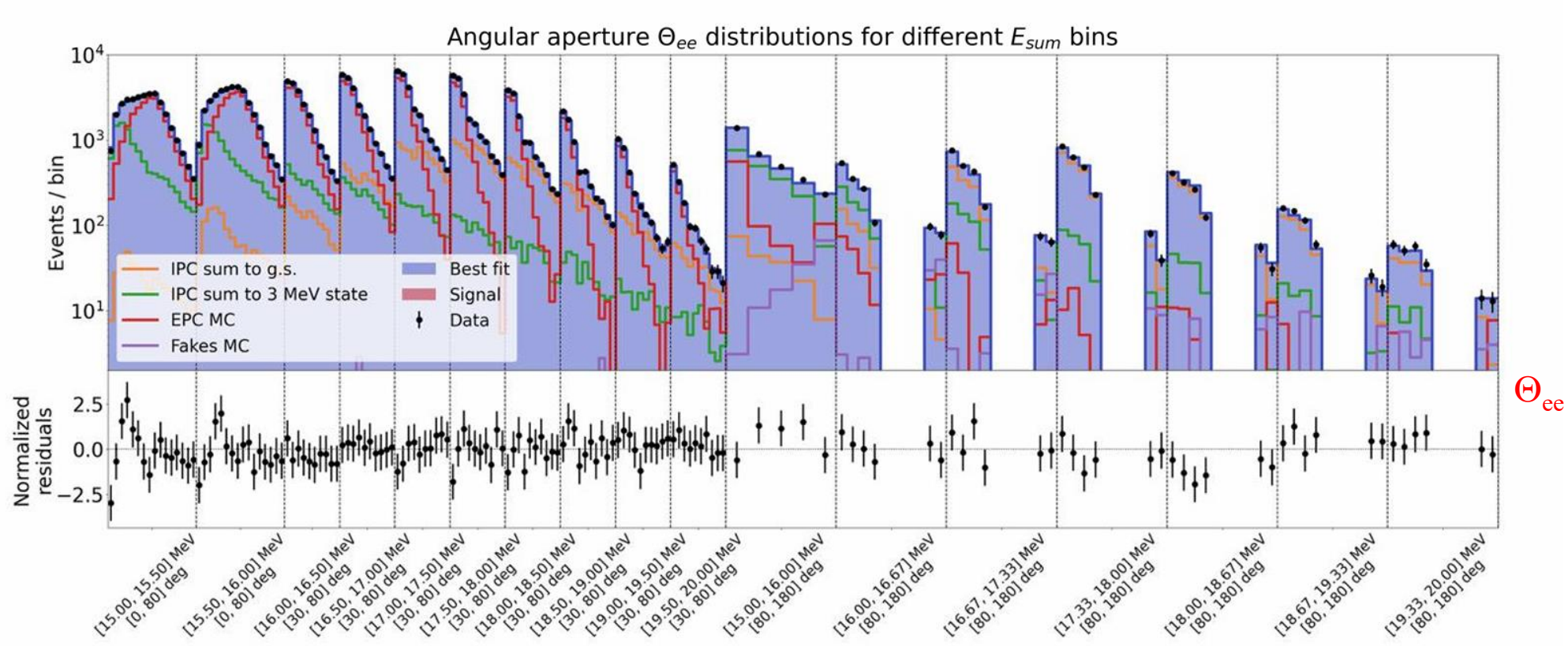

# Analysis strategy of the $e^+e^-$ signal

**Also several tests with toy Montecarlo experiments performed before unblinding**

**demonstrated that the fit could distinguish correctly**

**the contribution of the various backgrounds and the signals thanks to different shape in**

**the $E_{sum}$ - $\Theta_{ee}$ plane**

# Fit to the 2-D histogram, limited MC statistics

All the distributions generated by the Montecarlo were histograms in the $E_{sum}$ - $\Theta_{ee}$ plane with **limited statistics for many of the bins**.

**Practically unavoidable situation even when generating 100 million of MC events !**

To take into account that , modified the Likelihood according to a simplified Beeston-Barlow prescription

H. Dembinski and A. Abdelmotteleb
Eur. Phys. J C (2022) 82:1043

# Fit to the 2-D histogram, the hairy details

**The $E_{sum}$ $\Theta_{ee}$ plot was fitted by 10 MC distributions :**

IPC 18.1 MeV, IPC 15.1 MeV
IPC 17.6 MeV, IPC 14.6 MeV
} 2 resonance regions, distributions generated according to the Zhang-Miller model

IPC 17.9 MeV, IPC 14.9 MeV { nickname to mean the non-resonant region, covering the range $17.775 < E_{sum} < 18.05$ (IPC 17.9) or $14.775 < E_{sum} < 15.05$ (IPC 14.9); generated according to Zhang-Miller

EPC 18 MeV
EPC 15 MeV
} 2 distributions generated by GEANT4

X17 from 18.1 MeV resonance
X17 from 17.6 MeV resonance
} 2 distributions depending continuously on $M_{X17}$ via interpolation of templates
the X17 is assumed to decay isotropically in its c.m.s.

**….. plus one distribution for the fake pairs distribution**

**….. including also :** $k(M_{X17}) \equiv \frac{\varepsilon_{X17}(M_{X17})}{\varepsilon_{IPC}}$ } ratio of the X17 and IPC detection efficiency depending continuously on $M_{X17}$ via interpolation of templates

**….. including also :** a parameter $\alpha_{field}$ (it turned out to be close to 1) multiplying the value of the nominal magnetic field to take into account the uncertainty on it. It affects only the $E_{sum}$ distributions.

# Fit to the 2-D histogram, the hairy details

**….. including also :** the parameters corresponding to the simplified **Beeston-Barlow coefficients**, to take into account the MC limited statistics

**Further constraints :**

based on the BGO measured γ spectra. From theory we know that the cross section of γ's production have essentially the same shape of those of $e^+e^-$ production. That allows for the following constraints

$$N_{IPC17.6}/(N_{IPC14.6} + N_{IPC17.6}) = 66.3 \pm 1.7\ \%$$

$$N_{IPC17.9}/(N_{IPC14.9} + N_{IPC17.9}) = 48.2 \pm 1.9\ \%$$

$$N_{IPC18.1}/(N_{IPC15.1} + N_{IPC18.1}) = 43.0 \pm 2.0\ \%$$

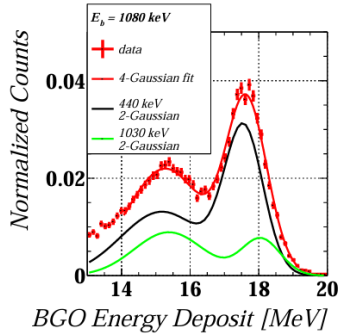


The **constraint terms**, and $\alpha_{field}$ and $k(M_{X17})$ were included in the Likelihood through gaussian terms.

Number of parameters in the fit : 13 parameters plus all the Beeston-Barlow coefficient parameters

# Unblinding

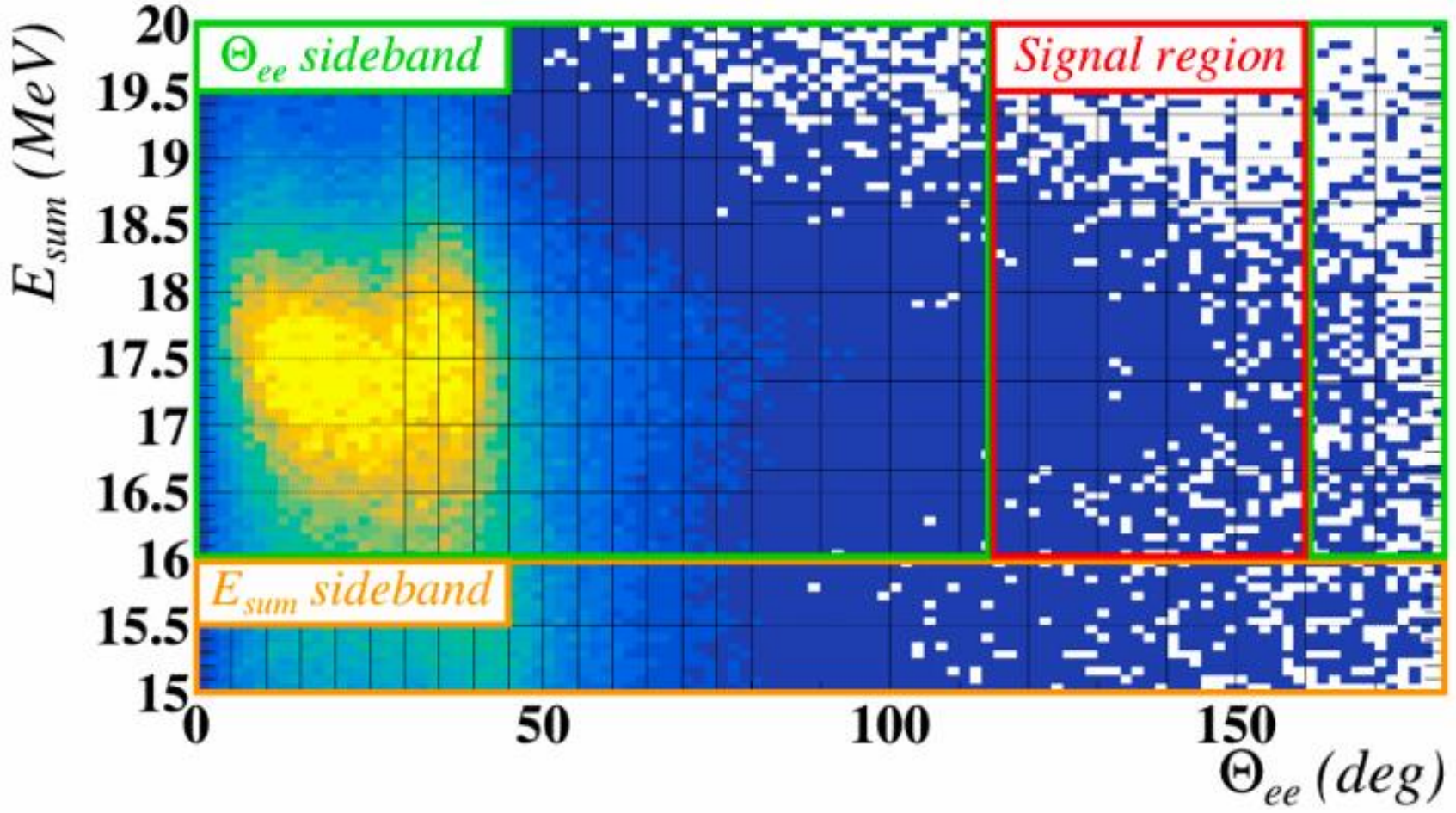
$\Theta_{ee}$ sideband
Signal region
$E_{sum}$ sideband
$E_{sum}$ (MeV)
20
19.5
19
18.5
18
17.5
17
16.5
16
15.5
15
0
50
100
150
$\Theta_{ee}$ (deg)

# Best fit results, no X17 events

$M_{X17}$ = 16.5 MeV

events X17 at 18.1 MeV = 10 ± 92 events
events X17 at 17.6 MeV = 0 ± 68 events
} no X17 events from fit

percentage of the IPC events : IPC 17.6 = ( 45.8 ± 1.3 ) % ; IPC 17.9 = 0 % ; IPC 18.1 = 12.6 ± 0.9 %

**godness of fit : p-value = 10.5 %** , calculated with toy montecarlos

Results shown in slices of $E_{sum}$ and $\Theta_{ee}$

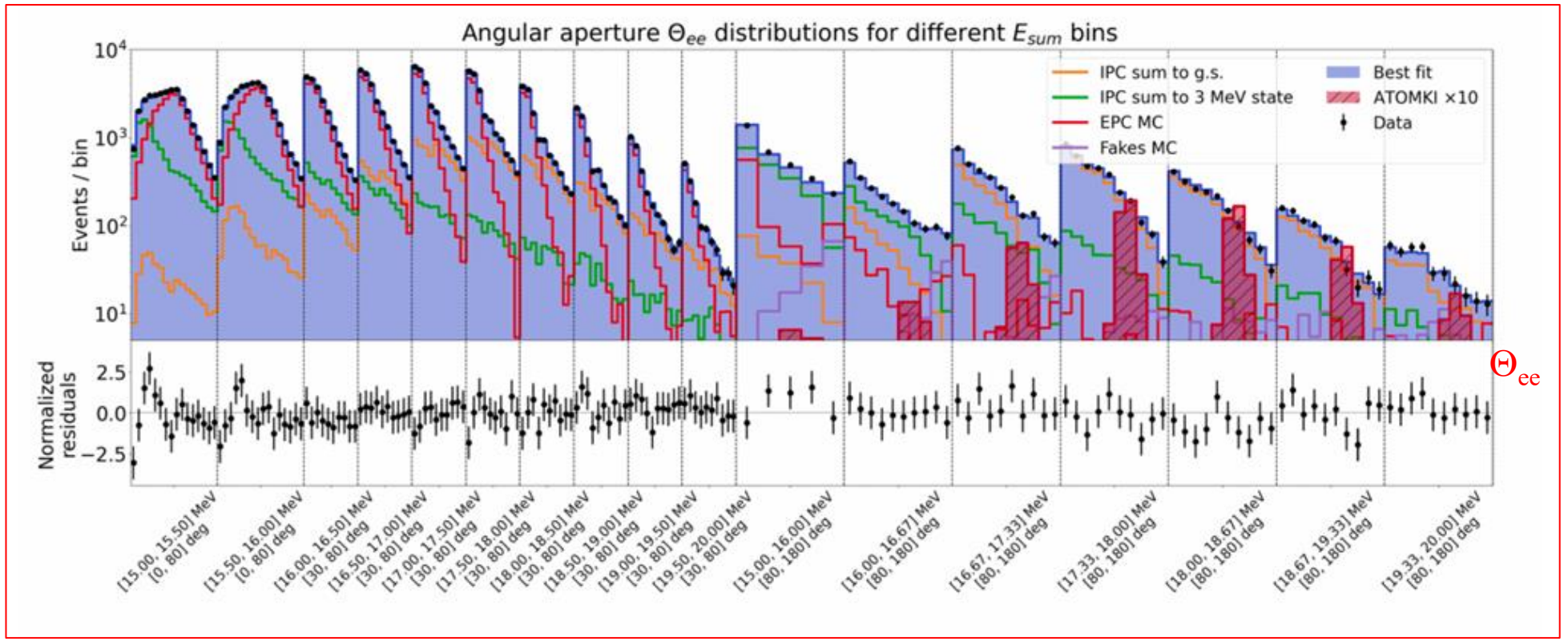

# the fit proves the 18.1 contribution is there

The MC distribution of the 18.1 and 17.6 MeV resonances projected in the $\Theta_{ee}$ axis in the signal region **were different enough** so that their contributions **could be evaluated by the fit with small errors.** The experimental data shape is different from the 17.6 shape and that **clearly demonstrates that a 18.1 contribution is there.**

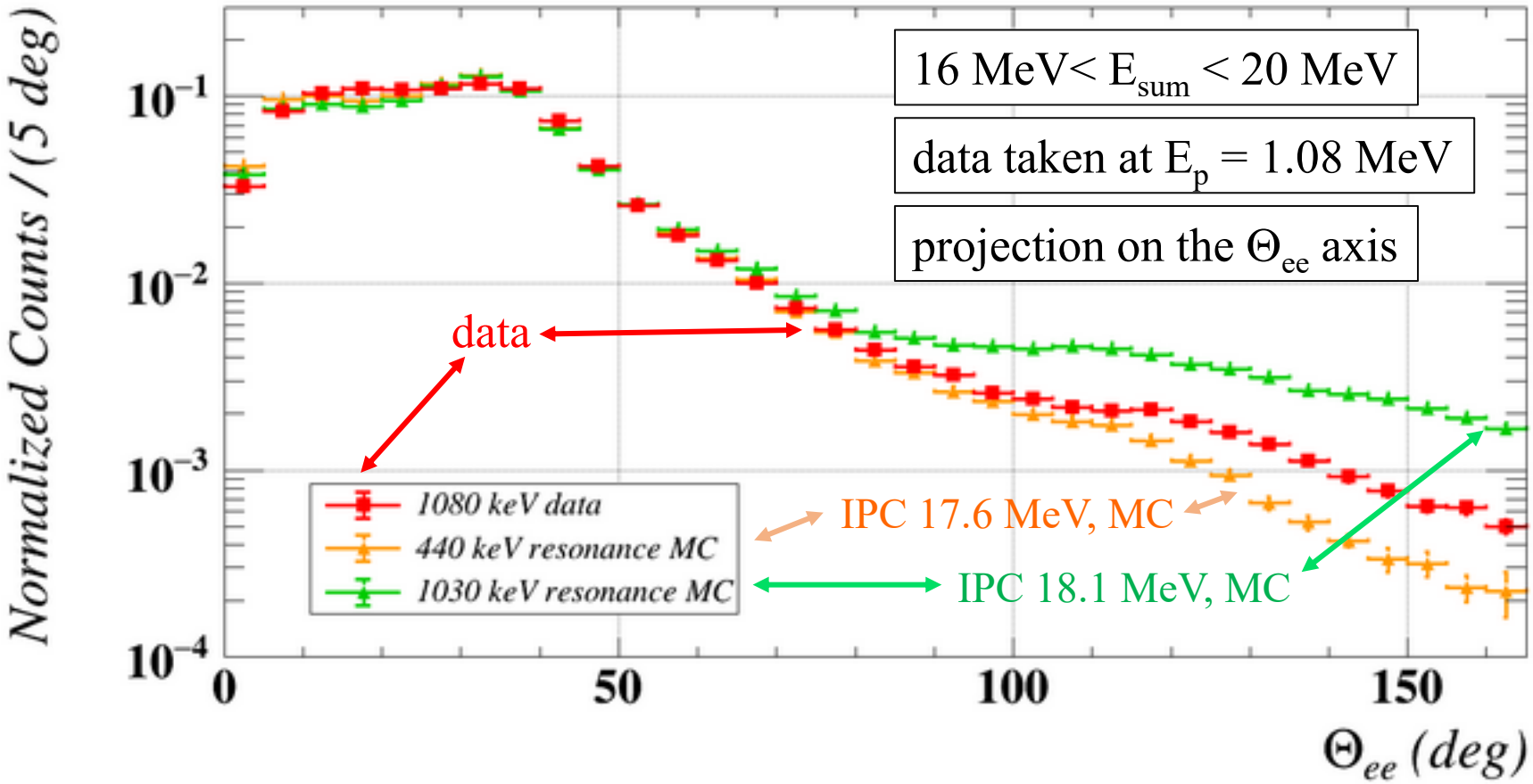

# 90 % CL upper limits

**The upper limits were calculated for the three parameters of physical interest :**

$$R_{18.1} \equiv \frac{\mathscr{B}(\,^{8}\mathrm{Be}^{*}(18.1\ \mathrm{MeV}) \rightarrow\ ^{8}\mathrm{Be} + \mathrm{X17})}{\mathscr{B}(\,^{8}\mathrm{Be}^{*}(18.1\ \mathrm{MeV}) \rightarrow\ ^{8}\mathrm{Be} + \gamma)}$$

$$\left(\frac{\mathscr{B}(\,^{8}\mathrm{Be}^{*}(18.1\ \mathrm{MeV}) \rightarrow\ ^{8}\mathrm{Be} + e^{+}e^{-})(IPC)}{\mathscr{B}(\,^{8}\mathrm{Be}^{*}(18.1\ \mathrm{MeV}) \rightarrow\ ^{8}\mathrm{Be} + \gamma)} = 3.9 \times 10^{-3}\right.$$
assumed from ATOMKI)

$$R_{17.6} \equiv \frac{\mathscr{B}(\,^{8}\mathrm{Be}^{*}(17.6\ \mathrm{MeV}) \rightarrow\ ^{8}\mathrm{Be}\ +\ \mathrm{X17})}{\mathscr{B}(\,^{8}\mathrm{Be}^{*}(17.6\ \mathrm{MeV}) \rightarrow\ ^{8}\mathrm{Be}\ +\ \gamma)}$$

$$\left(\frac{\mathscr{B}(\,^{8}\mathrm{Be}^{*}(17.6\ \mathrm{MeV}) \rightarrow\ ^{8}\mathrm{Be} + e^{+}e^{-})\ (IPC)}{\mathscr{B}(\,^{8}\mathrm{Be}^{*}(17.6\ \mathrm{MeV}) \rightarrow\ ^{8}\mathrm{Be} + \gamma)} = 3.4 \times 10^{-3}\right.$$
assumed from ATOMKI+Zhang-Miller model)

$M_{X17} \equiv$ mass of X17

# 90 % CL upper limits

Likelihood explicitly parametrized in terms of $R_{18.1}$ , $R_{17.6}$ and $M_{X17}$ . All the other parameters were considered as 'nuisance' parameters.

90% CL upper limits calculated for $R_{18.1}$ , $R_{17.6}$ and $M_{X17}$ using a 3-dimensional confidence region constructed according to Feldman-Cousins prescription.

Ordering based on $\lambda(R_{17.6}, R_{18.1}, M_{X17})$ ≡ profiled likelihood ratio :

$$\boldsymbol{\lambda(R_{17.6}, R_{18.1}, M_{X17}) = \frac{\mathcal{L}(R_{17.6}, R_{18.1}, M_{X17}, \hat{\hat{\eta}})}{\mathcal{L}(\hat{R}_{17.6}, \hat{R}_{18.1}, \hat{M}_{X17}, \hat{\eta})}}$$

$\mathcal{L}$ ≡ likelihood

η ≡ 'nuisance' parameters

$\hat{}$ , $\hat{\hat{}}$ ≡ indicate the variables with respect to which the likelihood is maximized

# 90 % CL upper limits

**3-D 90% confidence region calculated for**
**16.5 MeV < $M_{X17}$ < 17.1 MeV**

$R_{17.6} < 1.8 \times 10^{-6}$ $\quad N_{17.6}^{sig} < 200$

$R_{18.1} < 1.2 \times 10^{-5}$ $\quad N_{18.1}^{sig} < 230$

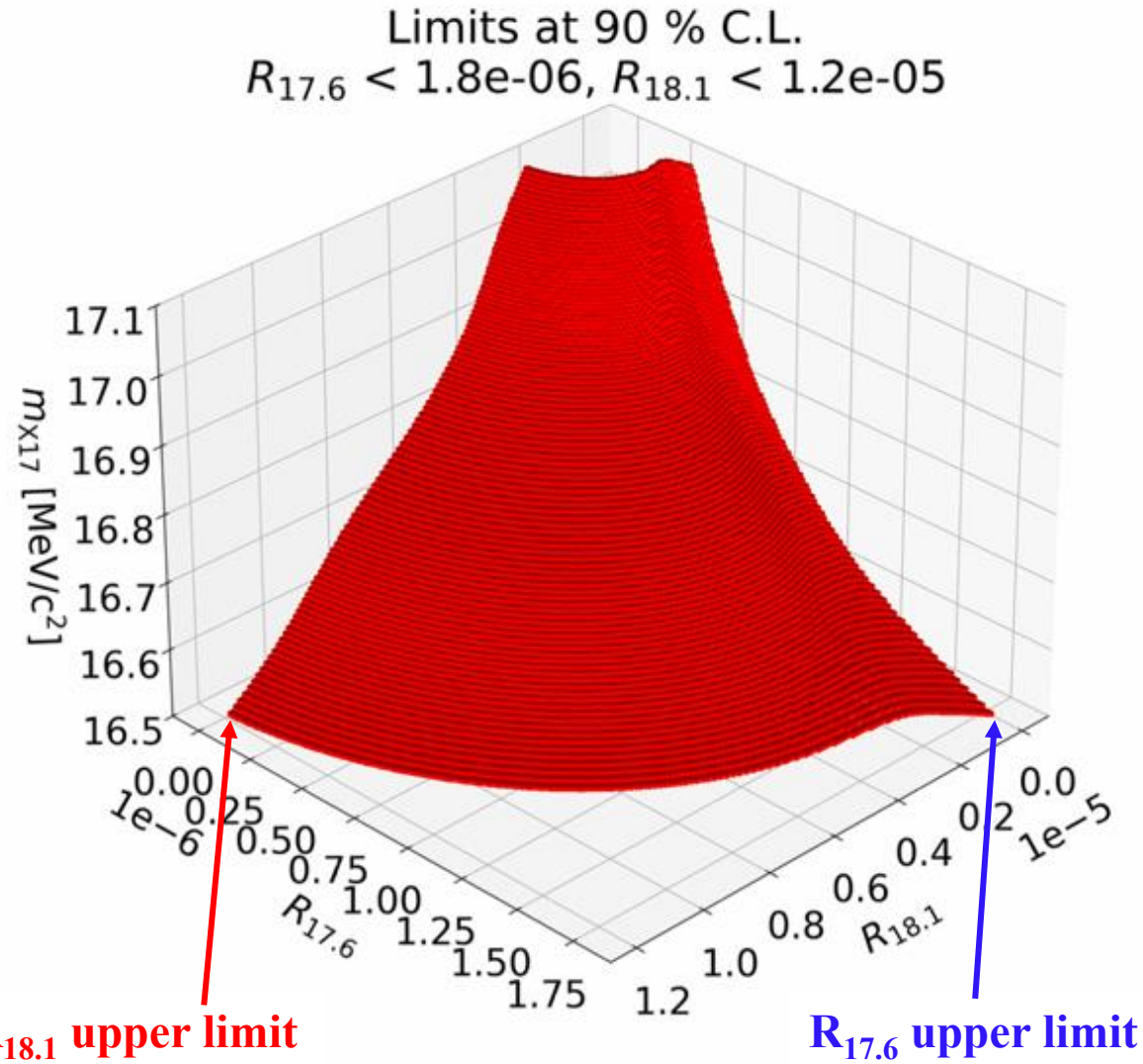

# 90 % CL upper limits projected

blue line : CL curve projected on the $R_{17.6}$ / $M_{X17}$ plane

red line : CL curve projected on the $R_{18.1}$ / $M_{X17}$ plane

ATOMKI average mass result from all channels :

$M_{X17} = 16.97 \pm 0.22$ MeV

$R_{18.1} = (6 \pm 1) \times 10^{-6}$

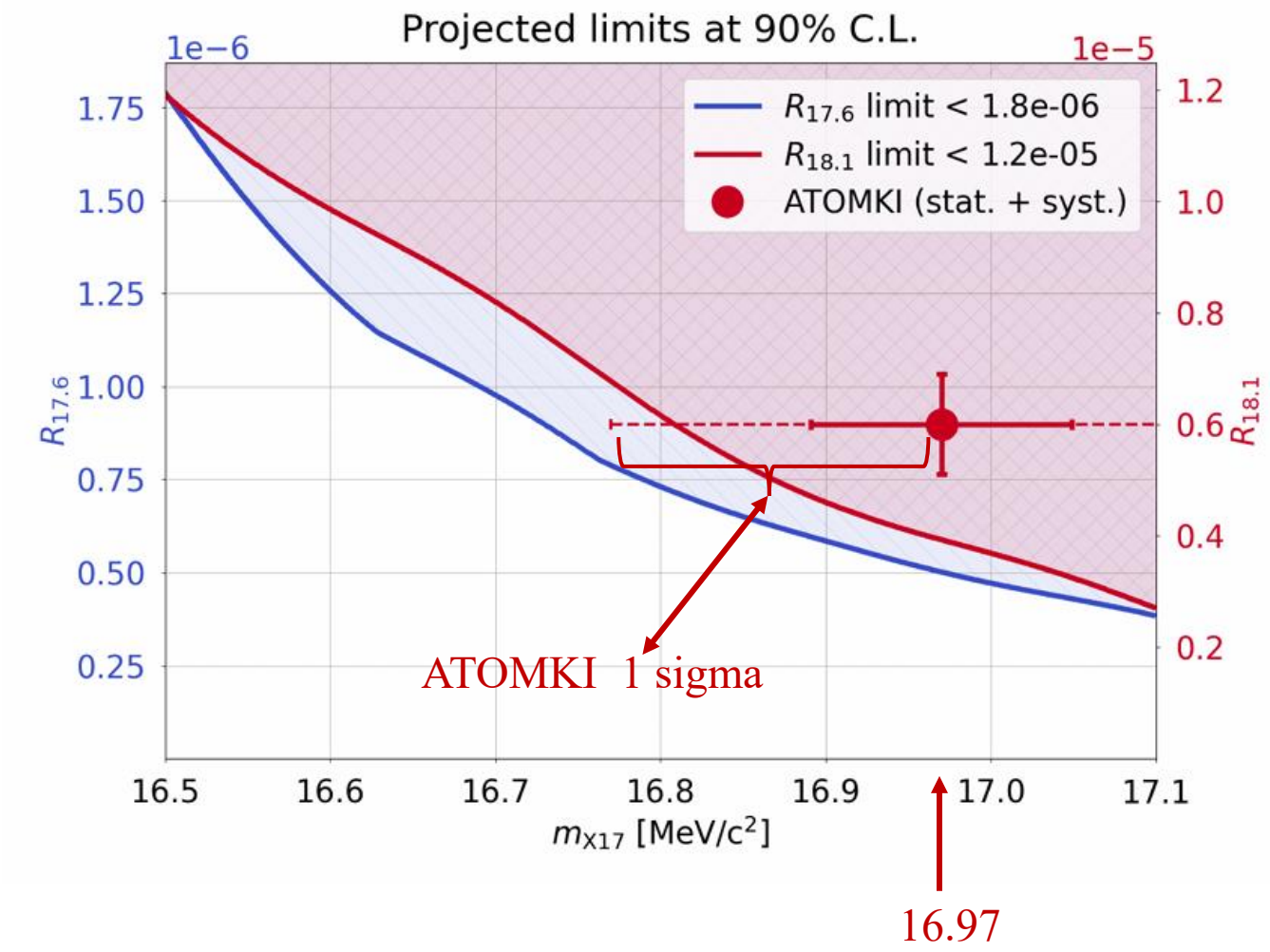

# Alternative hypothesis tests : compatibility of the ATOMKI hypothesis

'ATOMKI' hypothesis : X17 produced **only** from the decay $^{8}$Be*(18.1 MeV)

$M_{X17} = 16.97 \pm 0.22$ MeV $\qquad R_{18.1} = (6 \pm 1) \times 10^{-6}$ $\qquad R_{17.6} = 0$

Used the Profiled Likelihood ratio test of hypothesis :

$$\lambda_{ATOMKI} = \frac{\mathcal{L}\left(R_{17.6} = 0, R_{18.1} = 6 \text{ x } 10{-}6, M_{X17} = 16.97, \hat{\hat{\eta}}\right) G(M_{X17} = 16.97)}{\mathcal{L}\left(\hat{R}_{17.6}, \hat{R}_{18.1}, \hat{M}_{X17}, \hat{\eta}\right) G(\hat{M}_{X17})}$$

[ G($M_{X17}$ ) = gaussian constraint on $M_{X17}$ according to ATOMKI ]

…and then considered : $\mathbf{-2\ ln(\lambda_{ATOMKI})}$

In the large statistic limit $\mathbf{-2\ ln(\lambda_{ATOMKI}) = \chi^2_{\ ATOMKI}}$ with 3 degrees of freedom

# Alternative hypothesis tests : compatibility of the ATOMKI hypothesis 1

Using the MEG experimental data we obtain a -2 ln ($\lambda_{ATOMKI}$) such that its **p-value is 6.2 %**

[**p-value ≡ integral** of the -2 ln ($\lambda_{ATOMKI}$) ~ $\chi^2$ ATOMKI probability distribution function from the value obtained with the experimental data to infinity]

That means that the ATOMKI is compatible with the MEG result only if one accepts a confidence level of the test of **100% - 6.2 % = 93.8 % or more**

**It is costumary in the community to use 95% or 99% as the confidence level necessary to exclude the alternative hypothesis so this test cannot exclude the ATOMKI hypothesis even though it is close to exclude it.**

# Alternative hypothesis tests : compatibility of the ATOMKI hypothesis 2

Same check but changing the constraints

$$N_{IPC17.6}/(N_{IPC14.6} + N_{IPC17.6}) = 66.3 \pm 1.7\ \%$$

$$N_{IPC17.9}/(N_{IPC14.9} + N_{IPC17.9}) = 48.2 \pm 1.9\ \%$$

$$N_{IPC18.1}/(N_{IPC15.1} + N_{IPC18.1}) = 43.0 \pm 2.0\ \%$$

and setting them according to literature [Zahnow *et al*, Zietschrift für Physik A, Hadrons and Nuclei 351(2), 229 (1995) ]

The **p-value** of the distribution of **-2 ln $\lambda_{ATOMKI}$** in this test is **17.3%**

This means that the ATOMKI hypothesis 2 **is compatible** with the **MEG result** only if the **CL** required for the test **is 82.7 % or more**

# Alternative hypothesis tests : compatibility of the ‘Feng’ hypothesis

Same test for the **‘Feng’ hypothesis** :

X17 produced from the decay $^{8}$Be*(18.1 MeV) and $^{8}$Be*(17.6 MeV) with rates scaled according to J.Feng *et al*., Phys.Rev.Lett. 117(7), 071803 (2016)

**p-value = 1.8 % (2.1 σ) → ‘Feng’ hypothesis excluded at the 98.2 % level**

# Alternative hypothesis tests : compatibility of the ‘Feng’ hypothesis

Same check but changing the constraints

$$N_{IPC17.6}/(N_{IPC14.6} + N_{IPC17.6}) = 66.3 \pm 1.7\ \%$$

$$N_{IPC17.9}/(N_{IPC14.9} + N_{IPC17.9}) = 48.2 \pm 1.9\ \%$$

$$N_{IPC18.1}/(N_{IPC15.1} + N_{IPC18.1}) = 43.0 \pm 2.0\ \%$$

and changing them according to literature [Zahnow *et al*, Zietschrift für Physik A, Hadrons and Nuclei 351(2), 229 (1995) ]

**p-value = 1.2 % (2.3 σ) → ‘Feng’ hypothesis excluded at the 98.8 % level**

# Conclusions

The $^{7}Li + p \rightarrow {}^{8}Be\ e^{+}e^{-}$ process was studied with the MEG II detector at the Paul Scherrer Institute

Four weeks of dedicated data taking with a LiPON target and the MEG II Cockroft-Walton accelerator

Looking for the new particle X17 $\rightarrow$ $e^{+}e^{-}$ with mass ~ 17 MeV

No significant signal was found in our data in the best fit analysis ; ATOMKI hypothesis **compatible only if one requires a 93.8 % CL or more**

Upper Limits at 90% CL : $\mathbf{R_{18.1} < 1.2 \times 10^{-5}}$ $\mathbf{R_{17.6} < 1.8 \times 10^{-6}}$

for 16.5 MeV $< M_{X17} <$ 17.1 MeV